JOURNAL OF GEOPHYSICAL RESEARCH, VOL. 108, NO. E6, 5058, doi:10.1029/2002JE001962, 2003

A conceptual model for the relationship between coronae and large-scale mantle dynamics on Venus

Catherine L. Johnson
Institute of Geophysics and Planetary Physics, Scripps Institution of Oceanography, La Jolla, California, USA

Mark A. Richards
Department of Earth and Planetary Science, University of California, Berkeley, Berkeley, California, USA

Received 16 July 2002; revised 23 December 2002; accepted 18 February 2003; published 20 June 2003.

[1] Among the most enigmatic features on Venus are the more than 500 quasi-circular structures collectively referred to as coronae. Associated volcanism and tectonism suggest that coronae result from small, transient mantle plumes, although only about 20% have clearly associated positive gravity anomalies indicative of current activity. Coronae are concentrated within a region defined by the dynamically active highland areas of Beta, Atla, and Themis Regiones (BAT). Coronae avoid the lowest or highest topography and geoid. Subsets of the corona population indicate that the spatial distribution of coronae has evolved from a previously less concentrated global distribution to the current BAT concentration. Recent laboratory experiments on thermal convection at high Rayleigh number, using fluids with temperature-dependent viscosity, suggest a straightforward interpretation of these relationships. Small-scale upwellings from a hot lower thermal boundary layer tend to be excluded by longer-wavelength downwelling structures from the cold upper boundary layer. The relative paucity of coronae in the broad lowland plains regions is consistent with the inference of mantle downwellings beneath the plains. Coronae are largely excluded from compensated highlands, perhaps because the thickened crust is not easily disrupted in these regions. Laboratory experiments indicate that small, transient, boundary layer instabilities can coexist with, and be focused toward, large-scale upwellings, possibly explaining the spatial concentration of coronae in the BAT region. Thus coronae provide important insights into interacting scales of convective flow in Venus's mantle and into the evolution of Venus's mantle dynamics. Direct tests of our model are possible through geological mapping. *INDEX TERMS:* 5430 Planetology: Solid Surface Planets: Interiors (8147); 5475 Planetology: Solid Surface Planets: Tectonics (8149); 6295 Planetology: Solar System Objects: Venus; 8121 Tectonophysics: Dynamics, convection currents and mantle plumes; 8122 Tectonophysics: Dynamics, gravity and tectonics; *KEYWORDS:* Venus, coronae, gravity, tectonics, mantle dynamics, mantle plumes

Citation: Johnson, C. L., and M. A. Richards, A conceptual model for the relationship between coronae and large-scale mantle dynamics on Venus, *J. Geophys. Res.*, *108*(E6), 5058, doi:10.1029/2002JE001962, 2003.

1. Introduction

[2] NASA's Magellan mission to Venus (1989–1994) produced a wealth of data about Earth's sister planet, enabling previously unprecedented descriptions of its physiography and surface geology, and prompting new insights into the planet's internal dynamics and evolution. Altimetry and synthetic aperture radar (SAR) image data collected by Magellan [*Ford and Pettengill*, 1992] permit a first-order characterization of Venusian physiography (Figure 1a). Prominent in the global topography are long-wavelength highland and lowland regions. Highland regions include plateau-like features and long-wavelength topographic rises, somewhat analogous to hot spot rises on Earth. Plateau-like features are approximately 1–2 km in elevation above the mean radius (6051.9 km), and most have highly deformed surfaces: these are the so-called tessera such as Ovda Regio and Thetis Regio. Geoid anomalies associated with these features are typically positive (Figure 1b) and the variation of geoid (or gravity) with topography as a function of wavelength (admittance spectra) is consistent with isostatic support of the plateau topography due to thickened crust [*Simons et al.*, 1994; *McKenzie*, 1994]. The long-wavelength topographic rises are often cut by rift valleys: Beta and Atla Regiones are examples. These highland regions have large associated positive geoid and gravity anomalies (Figure 1b), and their admittance spectra (variation of gravity with topography as a function of wavelength) are consistent with dynamic support [*McKenzie*, 1994; *Phillips*,

0148-0227/03/2002JE001962$09.00

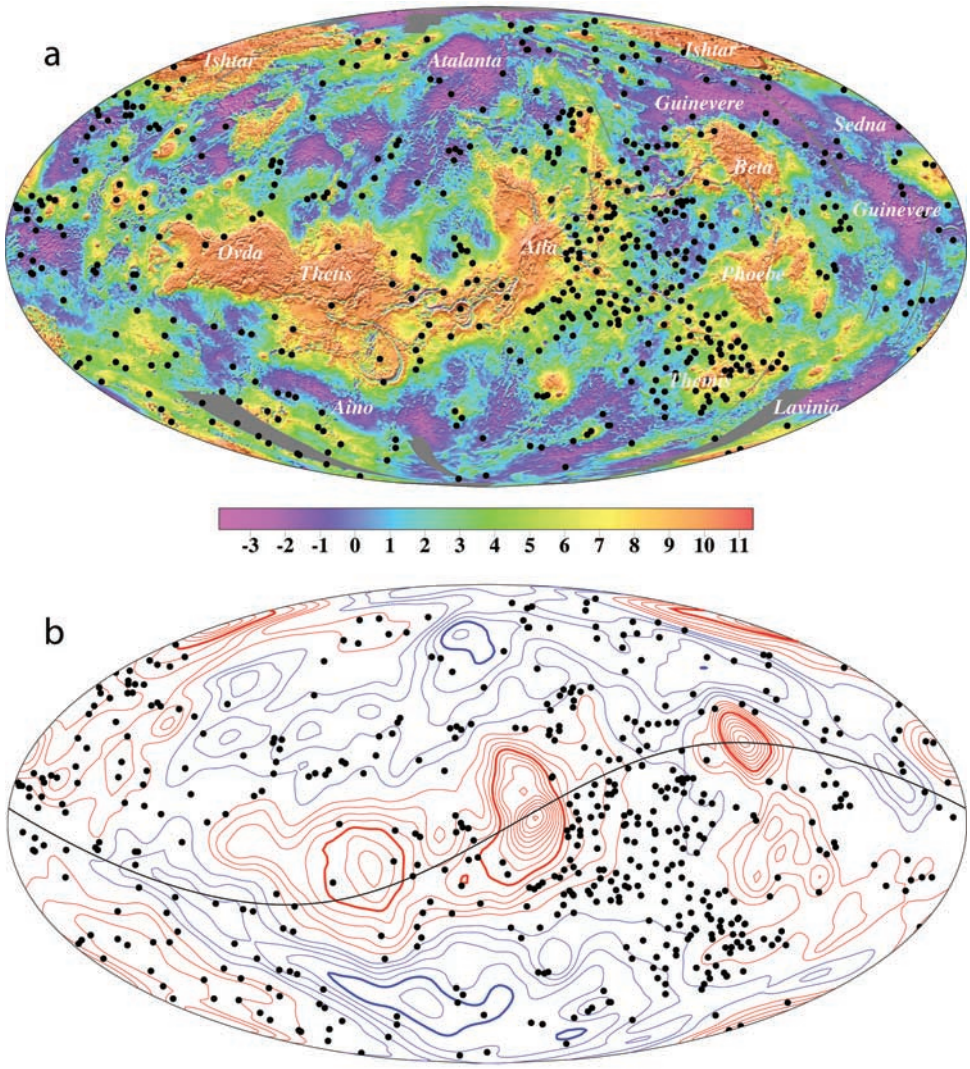

Figure 1. (a) Corona distribution [*Stofan et al.*, 2001] superposed on Venus topography. Hammer-Aitoff equal-area projection, centered on 180° longitude. Scale bar indicates topography in km about the mean elevation (6051.9 km). Gray areas are gaps in altimetry coverage. Names refer to major features. (b) Spherical harmonic expansion of geoid model MGN180USAAP [*Konopliv et al.*, 1999]. Geoid is low-pass filtered and contoured at 10 m intervals (negative contours are blue; positive contours are red; zero contour not plotted; heavier lines denote ±50 m contour). Corona distribution as in (a). The solid black line traces a great circle on the Venusian surface that forms the basis for the schematic cartoon in Figure 8.

1994; *Smrekar*, 1994; *Simons et al.*, 1997], likely related to large-scale mantle upwellings. Phoebe Regio appears to have elements of both types of highland regions [*Hansen et al.*, 1997; *Simons et al.*, 1997]. The surfaces of lowland regions are primarily smooth volcanic plains, and these lowland regions have large associated negative geoid and gravity anomalies (Figure 1b). On the basis of topography and gravity, the lowlands are interpreted to overly large-scale mantle downwellings [*Simons et al.*, 1997].

[3] One of the most surprising discoveries of the Magellan mission is the small number (939) of impact craters on the surface of Venus. Equally puzzling is the lack of geographical concentration of craters; unlike the Moon, Mercury or Mars, there are no old, heavily cratered surfaces exposed on Venus. The global distribution of impact craters is indistinguishable from a spatially random population [*Phillips et al.*, 1992; *Strom et al.*, 1994], suggesting a mean surface age for the planet of 700–800 Myr [*McKinnon et al.*, 1997]. Early interpretations of the cratering record focused on a dramatic paradigm: global (or catastrophic) resurfacing over a short time interval, with negligible resurfacing since that event [*Parmentier and Hess*, 1992; *Schaber et al.*, 1992; *Strom et al.*, 1994; *Turcotte*, 1993; *Turcotte et al.*, 1999]. Subsequent analyses of the statistics and geographical distribution of impact craters [*Hauck et al.*, 1998], along with detailed geological mapping [see, e.g., *Guest and Stofan*, 1999], indicate a more gradual evolution than implied by the "catastrophic" hypothesis. It is clear, however, that Venus underwent a major change in volcanic and tectonic style over some period of

time, accompanied by substantial resurfacing of the planet, and that there is little surface record of Venusian geological evolution prior to that period.

[4] The most widespread indicator of Venus's resurfacing history is the presence of large areas of volcanic plains (known as "regional plains" [*Basilevsky et al.*, 1997, and references therein]). Regional plains comprise extensive smooth flows, but also present are smaller spatial scale constructs and associated extrusive volcanism [*Addington*, 2001, and references therein]. The stratigraphy and impact crater statistics both point to an extended period of plains emplacement [*Hauck et al.*, 1998; *Guest and Stofan*, 1999]. A substantial volume of plains material was likely emplaced early in the major resurfacing episode, as a result of large-scale mantle upwellings and pervasive mantle melting [*Phillips and Hansen*, 1998], but resurfacing has continued [*Hauck et al.*, 1998; *Guest and Stofan*, 1999; *Addington*, 2001]. The terms "plains" and "lowlands" are often used interchangeably in the Venusian literature. In this paper, we use the term "lowlands" to refer to the topographically low regions seen in Figure 1a, such as Guinevere, Sedna, and Atalanta Planitia. These planitia are also regions of volcanic plains. From a dynamical standpoint, the distinction between "plains" and "lowlands" is important since "plains" are the result of mantle melting associated with upwellings. Subsequent to emplacement of large volumes of plains material, the large-scale dynamics of the Venusian mantle have likely changed; the current low topography of the plains, along with the geoid signature over these regions, indicates present-day, large-scale mantle downwellings beneath these regions. The distinction between plains and lowlands is important since mapping indicates that while coronae occur in the plains, they do not occur in the lowest topography of the lowlands.

[5] Venus also displays features unique among the terrestrial planets known as coronae. Coronae are quasi-circular to circular volcano-tectonic features that were first identified in Venera 15/16 images [*Barsukov et al.*, 1984, 1986]. They have been characterized in detail using Magellan SAR image and topography data [*Stofan et al.*, 1992, 2001]. Coronae range in diameter from 60 km to over 2500 km and were originally identified via an annulus of closely spaced fractures and/or ridges, often associated with a topographic rim. *Stofan et al.* [1992] required a fracture annulus of more than 180° in arc for a feature to be classified as a corona. Under this classification, 336 coronae were identified. A recent study updates this earlier work. It includes a new type of corona that has topographic rims but lacks extensive fracture annuli and is thus difficult to identify in SAR images alone. The current corona population comprises a total of 515 features of which 409 are fracture annuli coronae and 106 are topographic coronae [*Stofan et al.*, 2001]. The geographical distribution of this new corona population is shown in Figures 1a and 1b.

[6] Extensive studies of coronae over the past decade include global volcanic, tectonic, and topographic classifications [*Stofan et al.*, 1992; *Smrekar and Stofan*, 1997], models for corona evolution [*Janes et al.*, 1992; *Squyres et al.*, 1992; *Stofan et al.*, 1992; *Koch and Manga*, 1996; *Smrekar and Stofan*, 1997; *Hansen*, 2003], regional mapping [e.g., *Basilevsky and Head*, 1998; *Copp et al.*, 1998; *Chapman and Zimbelman*, 1998], and geophysical investigations [*Johnson et al.*, 1997; *Smrekar and Stofan*, 1999]. Volcanic characteristics of coronae are interior and annuli small cones, shields, smooth plains, small calderas, and extrusive, volcanic flow fields. Tectonic characteristics include annuli, interior radial and/or concentric ridges and graben. Nine topographic classes of coronae have been identified [*Smrekar and Stofan*, 1997].

[7] On the basis of their circular shape and their volcanic and tectonic features, coronae are interpreted to be surface manifestations of small- to intermediate-scale, transient mantle upwellings. Early numerical models examined the predictions for topography and surface stresses of a rising mantle diapir impinging on the base of the lithosphere [*Janes et al.*, 1992; *Squyres et al.*, 1992; *Stofan et al.*, 1992]. Limitations of these models in explaining the range of corona characteristics stemmed from model approximations such as simplified thermal and viscosity structures. A more recent model incorporating temperature-dependent viscosity and a depleted mantle layer [*Smrekar and Stofan*, 1997] predicts important aspects of corona formation and evolution, such as the full spectrum of corona topographic classes, and the lack of correlation of some fracture annuli with corona rim topography. Coronae may also have contributed significantly to heat loss on Venus [*Smrekar and Stofan*, 1997].

[8] Studies of impact crater densities associated with corona surfaces have been used to suggest that, on average the surfaces of coronae are young compared with the mean Venusian surface age [*Price and Suppe*, 1994; *Price et al.*, 1996; *Namiki and Solomon*, 1994]. The applications of such studies, however, are limited by statistical problems in investigating subsets of the small crater population [*Campbell*, 1999]. Furthermore, it is unclear what an average surface age means in the context of subsurface processes leading to corona formation or in the context of individual corona evolution. (Inferences of average surface ages for coronae as a class tacitly assume that all features of geologically similar terrain are of the same age.)

[9] Regional geological mapping [*Copp et al.*, 1998; *Chapman and Zimbelman*, 1998; *Smrekar and Stofan*, 1999] suggests a complex evolutionary history for individual coronae, and the formation of coronae possibly during, and since, the period of major resurfacing. *Chapman and Zimbelman* [1998] postulate that coronae form either in conjunction with older plains units or are younger (occurring after the period of major resurfacing) and concentrated in the Beta-Atla-Themis (BAT) region. The inferred complex evolution of coronae is consistent with predictions for numerical calculations [*Smrekar and Stofan*, 1997]. As we shall see in this paper, a gross distinction between older coronae associated with the volcanic plains and younger coronae concentrated in the BAT region is supported by analysis of corona gravity signatures.

[10] Our study is motivated by the need to establish the role of coronae in Venusian dynamics over the time period for which we have a geological surface record (750 Myr). While the concentration of coronae in the BAT region [e.g., *Stofan et al.*, 1992, 1997] and an anticorrelation of coronae with inferred upwellings and downwellings [*Herrick and Phillips*, 1992] have been noted, relationships between

coronae and large-scale interior dynamics of Venus have not been addressed in detail from an observational and theoretical perspective. *Herrick and Phillips* [1992], for example, inferred that coronae are the consequence of passive mantle upwelling, but that the association with mantle convective features is difficult to ascertain. Recent analogue laboratory experiments [*Weeraratne and Manga*, 1998; *Schaeffer and Manga*, 2001; *Lithgow-Bertelloni et al.*, 2001; *Jellinek et al.*, 2003] provide new insights into the temporal and spatial relationships between small-scale plumes and larger-scale dynamics in a convecting system. These experiments suggest straightforward interpretations of the observed spatial distribution of coronae on Venus.

[11] In this paper, we investigate the spatial distribution of coronae and its relation to long-wavelength features in the geoid and topography indicative of current or recent mantle processes. We also examine subsets of coronae that may be grossly representative of coronae formed during an era in which the large-scale mantle dynamics was different from that of the present-day. We review pertinent aspects of mantle convection theory and recent numerical studies, along with relevant laboratory experiments. We tie the major results to corona observations and inferences and suggest a hypothesis for the relation of coronae to larger-scale dynamical processes. We also outline potential future geological and numerical tests of our hypothesis.

2. Spatial Distribution of Coronae

[12] A recent study of the corona population documents 409 coronae with fracture annuli (known as Type 1 coronae) and 106 topographic (or Type 2) coronae [*Stofan et al.*, 2001]. The *Stofan et al.* [2001] database contains a duplicate entry as noted by *Glaze et al.* [2002]. The revised full coronae population (514 coronae) is shown in Figures 1a and 1b. Figure 1a shows the concentration of coronae in the Beta-Atla-Themis (BAT) region [*Stofan et al.*, 1992, 1997, 2001]. The remaining coronae occur largely in clusters forming topographic rises, and as isolated features in the volcanic plains regions, but avoiding the lowest topography in these regions (Guinevere, Sedna, Atalanta, Lavinia, and Aino Planitia). There is a relative deficit of coronae in the longitude region 100°E–200°E [*Stofan et al.*, 2001]. Despite the corona concentration in the BAT region, coronae are notably absent from the long-wavelength topographic highs of Beta, Atla, and Phoebe. Coronae also avoid the plateaus of Ovda, Thetis, Ishtar, and Tellus.

[13] Figure 1b shows the geoid derived from the degree and order 180 spherical harmonic model MGN180USAAP [*Konopliv et al.*, 1999]. A low-pass filter has been applied to ensure that features shown in the figure are resolvable. (Venus gravity field models have spatially varying resolution: in some regions, wavelengths as short as 300 km are resolvable, whereas in other regions, only wavelengths longer than 1000 km are resolvable.) In the low-pass filter, spherical harmonic degrees 2–30 are fully retained and a Gaussian roll-off is applied to degrees 30–60 (corresponding to wavelengths 1300 km–650 km). As with the topography, coronae avoid extreme geoid highs and lows. Only 6 out of 514 coronae occur in regions where the geoid has a magnitude greater than 50 m. There is no apparent correlation of the corona distribution with the geoid. Thus coronae avoid long-wavelength topographic highs and lows inferred to be supported by internal dynamics (either upwellings or downwellings), and they also tend to avoid long-wavelength topographic plateaus compensated by thickened crust [*McKenzie*, 1994; *Phillips*, 1994; *Simons et al.*, 1994; *Phillips et al.*, 1997]. While a direct comparison of the corona distribution with the geoid has not previously been published, *Herrick and Phillips* [1992] used a low-resolution (spherical harmonic degree and order 18), pre-Magellan model for the Venusian geoid [*Bills et al.*, 1987] and Pioneer Venus topography to infer mantle flow [*Richards and Hager*, 1984] and predicted the associated dynamic topography. From comparisons of their predicted dynamic topography and the corona data set of *Stofan et al.* [1992], *Herrick and Phillips* [1992] concluded that the spatial distribution of coronae was anticorrelated with high-amplitude upwellings and downwellings.

[14] Most corona studies to-date have investigated the Type 1 coronae. This population of coronae is thought to comprise coronae representing a wide range of stages of evolution on the basis of geological mapping and the comparison of topographic forms with the predictions of numerical models [*Smrekar and Stofan*, 1997]. We compare the spatial distributions of two subsets of the Type 1 coronae: compensated and uncompensated coronae (Figure 2). Uncompensated coronae have significant associated free air gravity anomalies; compensated coronae have no discernible gravity signature. Compensated coronae are inferred to be "older" features in the sense that any dynamical processes associated with corona formation have ceased.

[15] We then compare the distribution of the Type 1 coronae with the Type 2 coronae (Figure 3) [*Stofan et al.*, 2001]. As noted above, Type 1 coronae likely comprise coronae in a wide spectrum of evolutionary stages. In contrast, *Stofan et al.* [2001] suggested that many Type 2 coronae have topographic forms indicating they are in a relatively advanced stage of evolution. Comparison of properties of these two data sets enables us to test whether the Type 1 and 2 coronae are statistical samples from the same underlying spatial distribution. *Glaze et al.* [2002] have investigated corona size and topographic form for these two data sets. They find that the diameters of Type 1 and Type 2 coronae are consistent with sampling from the same underlying statistical distribution. However, *Glaze et al.* [2002] find differences in the dominant topographic morphology of the two subsets of coronae. Type 1 coronae typically occur as rimmed depressions, whereas Type 2 coronae most frequently occur with flat interiors and raised rims. Here we examine the geographical distributions of these subsets of coronae. Given the inferences of the broader and narrower range of stages of evolution of the Type 1 and 2 corona data sets respectively, investigations of the spatial distributions of these two subsets of the corona population may provide information on albeit gross average changes in spatial distribution with time.

[16] Figure 2 shows the distribution of uncompensated and compensated coronae. These data were compiled from a study of the *Stofan et al.* [2001] corona data set [*Zimmerman and Johnson*, 2000; *Johnson and Solomon*, 2002]. The gravity field (model MGN180USAAP) at each corona in the data set was examined and the peak anomaly over the corona recorded. Some coronae are too small relative to the

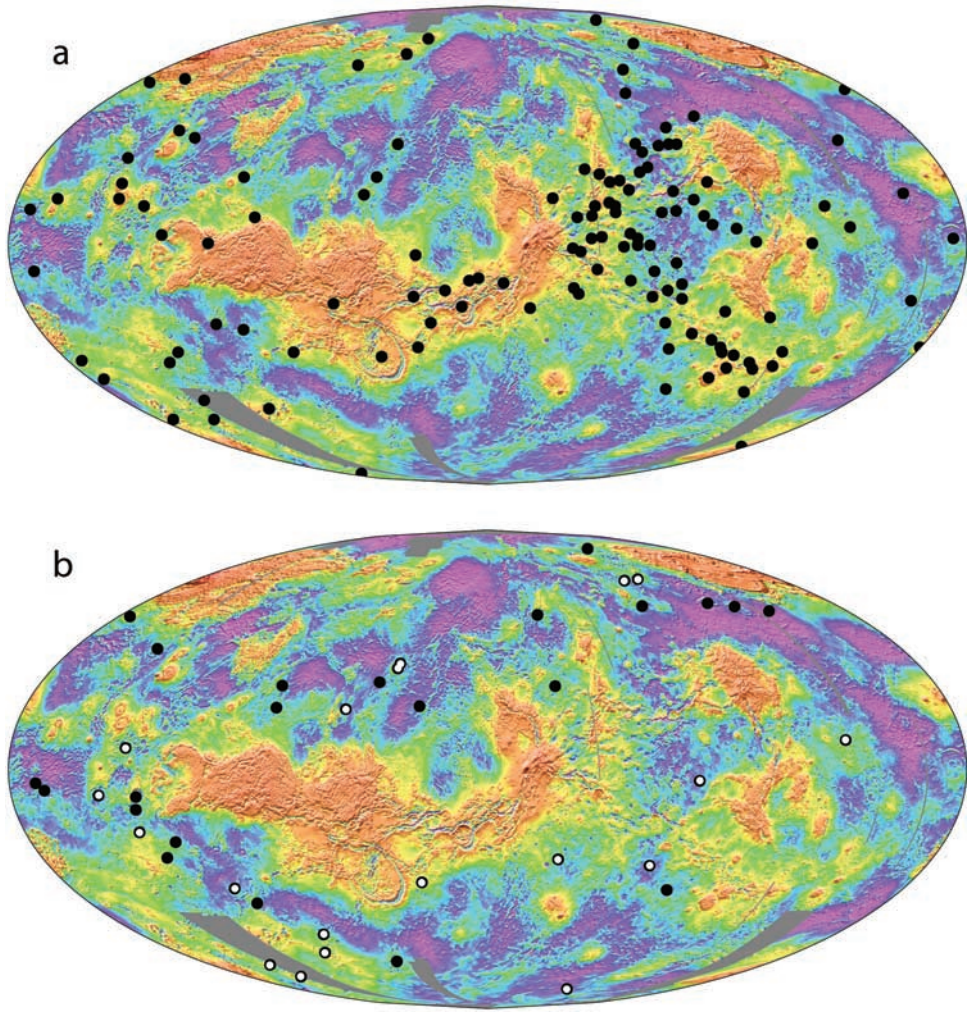

Figure 2. Geographical distribution of (a) uncompensated (N = 125) and (b) compensated (N = 41) total coronae superposed on topography. In Figure 2b, the filled black circles indicate the most robustly identified compensated coronae (N = 22), and the white circles indicate additional coronae (N = 19) that may be compensated. Projection and color scale as in Figure 1a.

resolution in the gravity field for an anomaly to be detected. The resolution in the gravity field at a particular location was taken from the degree strength map of *Konopliv et al.* [1999]. The degree strength map provides an estimate of the maximum spherical harmonic degree below which there is discernible power in the gravity field model. The equivalent minimum resolvable wavelength corresponding to the degree strength is calculated. A zero free air anomaly was taken to represent a compensated corona only if the corona has significant topographic relief and its maximum diameter is greater than half the minimum resolvable wavelength in the gravity field at that location. Using these criteria we recorded 22 clearly compensated and 125 uncompensated coronae (Figure 2). We also identified a further 19 coronae that may be compensated, but for which careful examination suggests that the resolution of the gravity field is possibly less than that indicated by the degree strength map leading to uncertainty in the interpretation of a zero free air anomaly (Figure 2). Of the 125 uncompensated coronae, 78 have a positive gravity anomaly. Clearly, these analyses are subject to the criteria used in establishing whether an individual corona is large enough and with sufficient relief to enable a non-zero gravity anomaly to be detected. Our investigations, however, show that changing the criteria slightly does not change the overall geographical distributions shown in Figure 2.

[17] The majority of uncompensated coronae are concentrated in the BAT region (Figure 2), with the remainder occurring as isolated features or forming the so-called ''corona-dominated rises'' [*Smrekar and Stofan*, 1999]. The BAT region (defined approximately here by latitudes 45°N and 45°S, and longitudes 195°E and 285°E) accounts for about thirty five per cent of the surface area of Venus. Forty per cent of the total corona population and fifty per cent of the uncompensated coronae occur in the BAT region. Compensated coronae appear to have no preferred concentrations in specific geographical regions. In particular, they show a notably low concentration in the BAT region. The absence of compensated coronae in the longitude band 120°–180°E reflects the paucity of coronae in general in this region, coupled with the poor gravity field resolution, especially for latitudes south of 20°N.

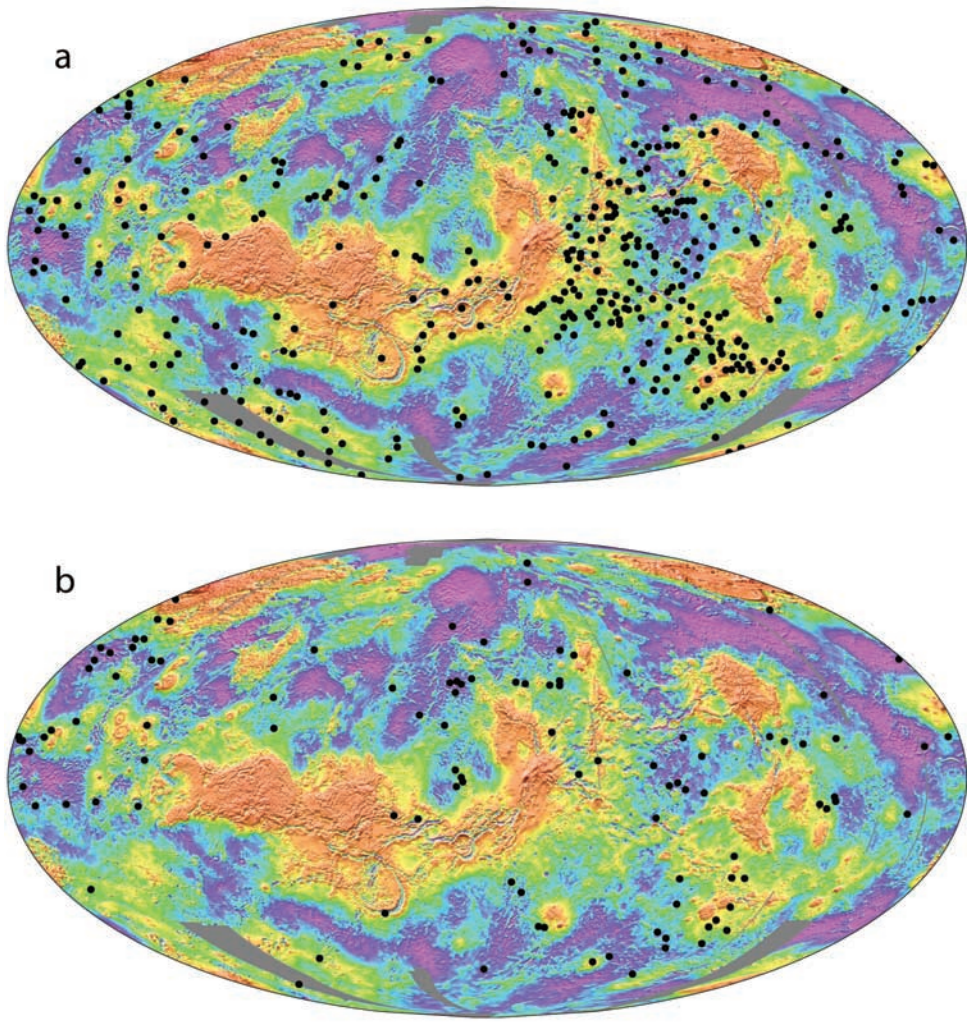

Figure 3. Geographical distribution of (a) Type 1 or fracture annuli (N = 408) and (b) Type 2 or topographic (N = 106) coronae [*Stofan et al.*, 2001] superposed on topography. Projection and color scale as in Figure 1a.

[18] Figure 3 shows the spatial distributions of Type 1 and Type 2 coronae [*Stofan et al.*, 2001]. The Type 1 coronae distribution (Figure 3a) reflects that of the complete corona data set, being concentrated in the BAT region, but also occurring in other regions. Type 2 coronae, however, do not appear to have a preferential concentration in the BAT region; only 21% of Type 2 coronae occur in this region. Although the Type 2 coronae appear to have a more uniform geographic distribution (Figure 3b) than Type 1 coronae, we shall see below that the Type 2 corona distribution is not compatible with a spatially random distribution.

3. Statistical Tests

[19] We are interested in whether subsets of the corona population indicate changes in the distribution of coronae over time. To address this question we have conducted statistical tests on both the spatial (this section) and spectral (next section) characteristics of the corona subsets.

[20] First we test whether any of the subsets of the corona population are consistent with the hypothesis that they are drawn from a spatially random distribution. We use a standard approach in analyzing distributions on a sphere: *Watson*'s [1956] test for randomness. For a random distribution of N unit vectors (representing a random distribution of points on a sphere), the resultant vector, R, will be small. For increased clustering, R will approach N. *Watson* [1956] defined a critical value, R_0, that can be used to test the randomness of a data set. If R exceeds R_0, the null hypothesis of randomness can be rejected at a specified confidence level. If R is less than R_0, randomness cannot be disproved. Table 1 gives the values for N, R, R_0 for the

Table 1. Watson's Test for Randomness

Corona Data Set	Number of Coronae, N	Resultant Vector, R	Test Statistic,[b] R_0
Type 1	407[a]	354.4	32.6
Type 2	106	93.5	16.6
Uncompensated	125	111.7	18.0
Compensated	22	19.0	7.6

[a]Artemis corona excluded from analyses, duplicate entry removed from *Stofan et al.* [2001].
[b]If $R < R_0$, randomness cannot be disproved.

Table 2. Kolmogorov-Smirnov Test

Data Sets Compared	K-S Statistic, D	Probability (D > Observed)
Uncompensated, Compensated	0.46	4.2×10^{-4}
Type 1, Type 2	0.30	3.2×10^{-7}

Type 1, Type 2, compensated and uncompensated corona data sets. At the 95% confidence level, none of the subsets of the corona population are consistent with being drawn from a random distribution.

[21] Next we tested whether the subsets of compensated and uncompensated coronae and of Type 1 and Type 2 coronae might be drawn from the same underlying distribution. We computed nearest neighbor angular distances between all pairs of coronae for the uncompensated coronae, compensated coronae, Type 1 coronae, and Type 2 coronae. The Kolmogorov-Smirnov test [*Press et al.*, 1989] allows us to compare the cumulative distribution function of the nearest neighbor distances for any two subsets of the corona population. One can determine whether it is possible (at a specified significance level) to reject the null hypothesis that the two subsets of data are drawn from the same underlying statistical distribution. One of the advantages of this test is that the form of the underlying statistical distribution need not be known. We have conducted Kolmogorov-Smirnov tests on nearest neighbor distances (angles) for the compensated versus uncompensated coronae and for the Type 1 versus Type 2 coronae (Table 2). For both comparisons the null hypothesis can be rejected at the 95% confidence level.

[22] In summary, the analyses above indicate that none of the compensated, uncompensated, Type 1 or Type 2 corona data sets are randomly distributed. The Type 1 and uncompensated coronae are concentrated in the BAT region. The hypothesis that the distributions of Type 1 and Type 2 and of uncompensated and compensated coronae are drawn from the same underlying population can be rejected at the 95% confidence level.

4. Spectral Analyses

[23] Spectral analyses provide an alternative (wave number domain) description of corona distributions and permit analyses of correlations among subsets of coronae, topography, and the geoid (or gravity). Spectral analyses allow us to quantitatively investigate characteristic length scales of behavior of distributions on a sphere.

4.1. Approach

[24] Spectral analyses of a scalar field described in spherical geometry, A(θ, ϕ), are enabled through a spherical harmonic description given by

$$A(\theta,\varphi) = \sum_{l,m} a_{lm} Y_{lm}(\theta,\varphi),$$

and

$$Y_{lm}(\theta,\varphi) = (-1)^m \sqrt{\frac{(2l+1)}{4\pi}\frac{(l-m)!}{(l+m)!}} P_{lm}(\cos(\theta)) \exp(im\varphi),$$

where θ is colatitude and ϕ is longitude, and P_{lm} is an associated Legendre polynomial of degree l and order m. Each spherical harmonic, Y_{lm}, is fully normalized such that

$$\int_0^{2\pi}\int_0^{\pi} Y_{lm} Y^*_{l'm'} \sin\theta d\theta d\varphi = \delta_{mm'}\delta_{ll'}$$

and the coefficients, a_{lm}, are referred to as the fully normalized spherical harmonic coefficients. The power spectrum as a function of spherical harmonic degree is calculated from

$$S_l = \frac{\sum_m a_{lm} a^*_{lm}}{2l+1},$$

where * denotes the complex conjugate. The degree-correlation between two fields A and B is given by

$$r_l = \frac{\sum_m a_{lm} b^*_{lm}}{\sqrt{\sum_m a_{lm} a^*_{lm} \sum_m b_{lm} b^*_{lm}}}.$$

Confidence intervals on the degree-correlation are calculated using the Student's t test [*Press et al.*, 1989].

[25] Spherical harmonic expansions were made of the 5 corona distributions shown in Figures 1–3. In subsequent analyses, we omit Artemis corona since it is anomalous in its size, its evolutionary history is poorly understood, and it is probably unique rather than typical of coronae as a class. Since we are interested in the long-wavelength components of the corona distributions, we restrict our spherical harmonic expansions to spherical harmonic degree and order 20 or less (equivalent to wavelengths longer than 1900 km).

4.2. Results

[26] As a starting point, we compare the power spectra for the full corona distribution with the corresponding long-wavelength components of the power spectra for the topography and geoid. We use spherical harmonic models TOPO360B [*Rappaport et al.*, 1999] and MGN180USAAP [*Konopliv et al.*, 1999] for the topography and geoid, respectively. The power spectra have been normalized to have equal power at spherical harmonic degree two so that the shape of the power spectra can be easily compared. As has been reported elsewhere [e.g., *Rappaport et al.*, 1999; *Konopliv et al.*, 1999], the geoid and topography fields have red power spectra (decreasing power at high spatial frequencies), although there is decreased power in the topography field at spherical harmonic degrees 1 and 2. The full corona data set has a red power spectrum at the longest wavelengths ($l < 10$) and an approximately white (constant power with spatial frequency) spectrum at shorter wavelengths. Correlations between these fields are shown in Figure 4b. Again, as previously reported, topography and geoid or gravity are extremely well correlated at all spherical harmonic degrees except $l = 2$ [*Phillips and Malin*, 1983; *Konopliv et al.*, 1999]. The corona distribution shows no significant correlation with either the geoid or topography for spherical harmonic degrees less than 20 (wave-

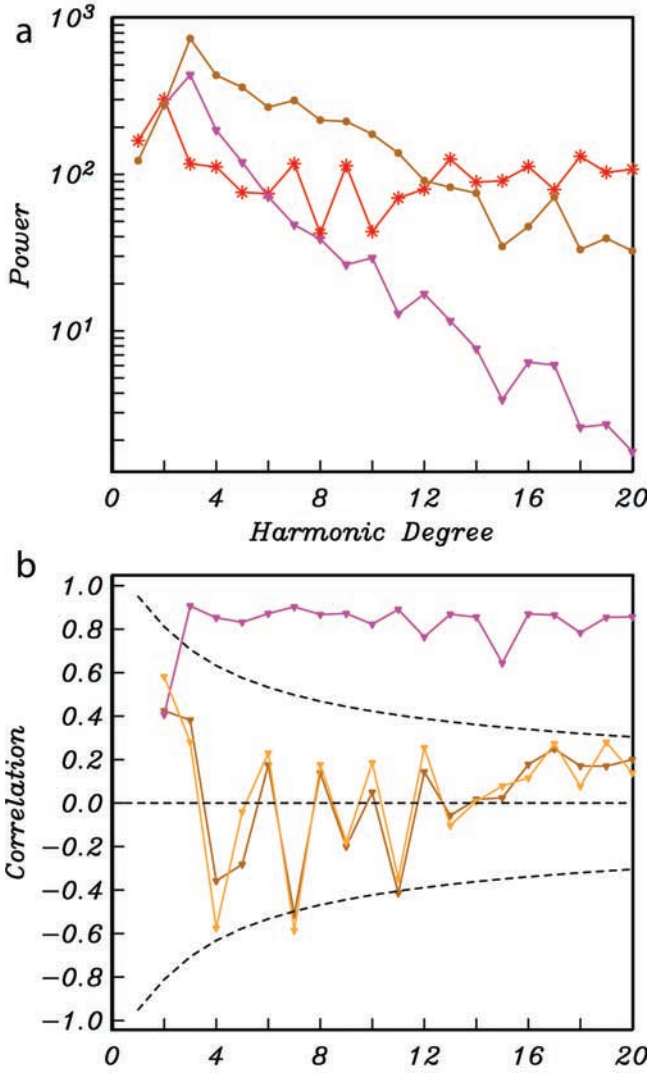

Figure 4. (a) Degree power spectra for all coronae (red), topography (brown), and geoid (purple). See text for details. Spectra are normalized to have the same power at spherical harmonic degree 2. (a) Correlation between topography and geoid (purple), topography and all coronae (orange), geoid and all coronae (brown).

lengths greater than 1900 km). This finding provides quantitative confirmation of the observations based on Figure 1.

[27] The power spectra and correlation for the compensated and uncompensated subsets of the corona data set are shown in Figures 5a and 5b, respectively. The uncompensated coronae show a red spectrum at spherical harmonic degrees less than eight, similar to that for the whole corona data set. For higher spherical harmonic degrees, the spectrum for the distribution of uncompensated coronae is white. In contrast, the compensated coronae show a blue spectrum for $0 < l < 20$ (increasing power with increasing spherical harmonic degree). Examination of the degree-correlation between the two spatial distributions shows no significant correlation.

[28] The power spectra and correlation for Type 1 and 2 coronae are shown in Figures 6a and 6b, respectively. The power spectra (Figure 6a) for Type 1 coronae mirrors that of the full corona data set, as would be proposed simply on a comparison of the spatial distributions shown in Figure 1 and Figure 3a. In contrast, Type 2 coronae have, on average, an almost white spectrum for spherical harmonic degrees less than 20. The Type 1 corona distribution is almost perfectly correlated with the full corona data distribution (Figure 6b). The Type 1 and Type 2 corona data sets are uncorrelated spatially for all spherical harmonic degrees less than 20, at the 95% confidence level.

5. Implications for the Internal Dynamics of Venus

[29] On Earth, the hot spot (mantle plume) distribution is strongly correlated with both long-wavelength geoid highs [e.g., *Crough and Jurdy*, 1980; *Richards et al.*, 1988] and

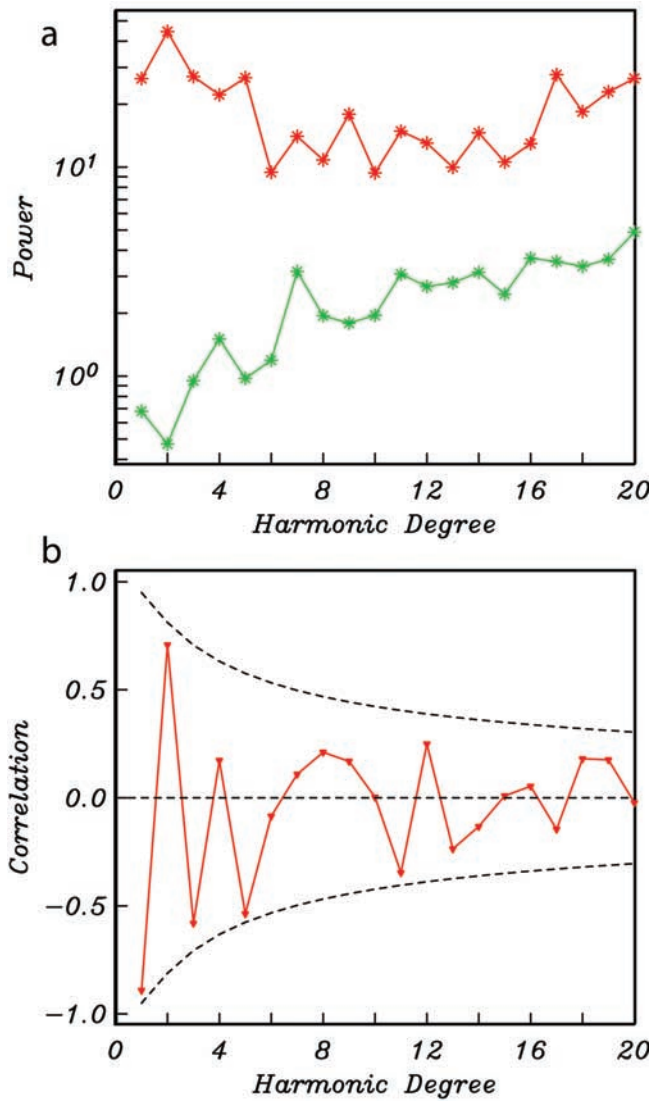

Figure 5. (a) Power spectra as a function of spherical harmonic degree for uncompensated (red) and compensated (green) coronae. (b) Degree correlation between uncompensated and compensated coronae. Dashed lines are 95% confidence limits for the correlation.

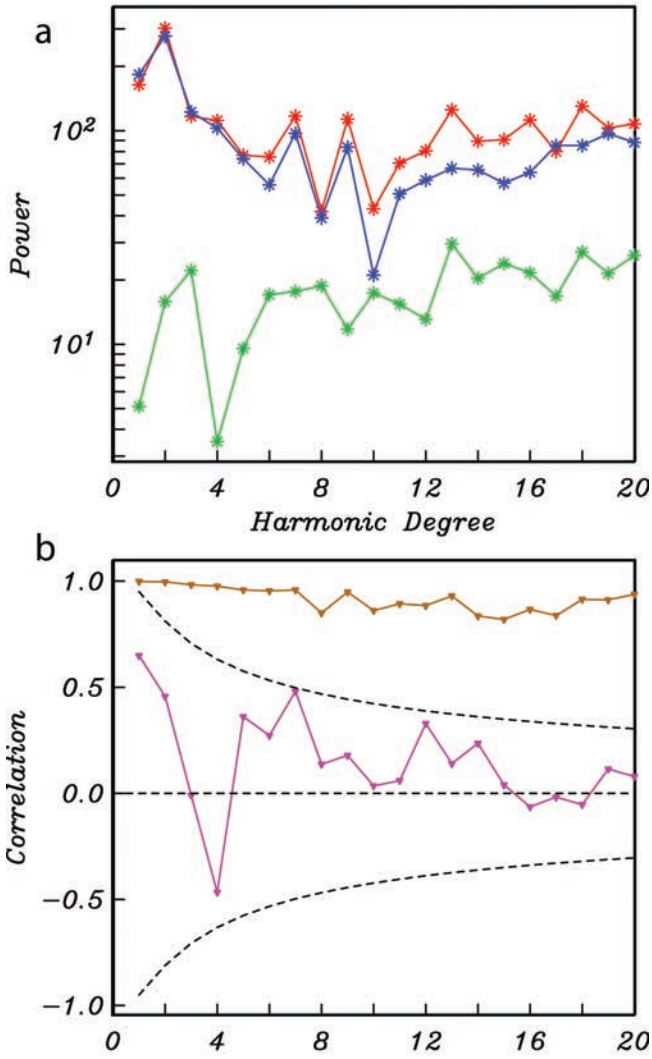

Figure 6. (a) Degree power spectra for all coronae except Artemis (red, N = 513), Type 1 coronae (blue, N = 407), Type 2 coronae (green, N = 106). (b) Degree correlation between Type 1 coronae and all coronae (brown), Type 1 coronae and Type 2 coronae (purple).

with seismic low-velocity anomalies in the deep mantle (mantle upwellings), and hot spots are anticorrelated with the time-integrated history of subduction (mantle downwellings) [*Richards and Engebretson*, 1992]. Hot spots are not correlated with long-wavelength topography, but this merely reflects the fact that Earth's topography is dominated by compensated crustal thickness variations (e.g., continent versus ocean) not generally associated with active mantle convection structures. The correlation of hot spots with geoid highs and low seismic velocity (along with hot spot fixity and geochemistry) has led to general acceptance that hot spots are associated with large-scale convection in the deep mantle, and that their source region is the lowermost mantle, near the core-mantle boundary.

[30] The contrasting lack of correlation of coronae with both long-wavelength topography and gravity on Venus might therefore be taken to suggest that the small-scale transient plume activity responsible for coronae is not strongly coupled to large-scale mantle convection. We, however, have reached quite the opposite conclusion from consideration of the dynamical nature of the various tectonic (topographic) provinces on Venus and their correlations with coronae distributions:

[31] 1. Coronae are largely excluded from broad lowland regions, such as Guinevere, Atalanta, Lavinia, and Aino (see Figure 1a). These lowland volcanic plains regions exhibit uncompensated geoid lows (Figure 1b), which suggests that they overlie present-day broad downwellings of cold lithosphere [*Simons et al.*, 1997]. It is reasonable to conclude that hot boundary layer instabilities that generate transient plumes are suppressed beneath such downwelling regions and that coronae are therefore generally excluded from such regions, similar to the above-noted exclusion of hot spots on Earth from regions of past and present subduction. This is consistent with the paucity of uncompensated coronae in lowland areas. The few uncompensated coronae present in these regions may reflect occasional transient instabilities from the lowermost mantle, that are able to reach the surface.

[32] 2. Coronae are also largely absent from compensated highland plateaus, which probably represent relatively old and thickened crust and may or may not be underlain by active thermal structures, in contrast to the active highlands and lowlands of Venus. The compensated highlands may exclude coronae either (a) because it is difficult for the signatures of transient plumes to penetrate thickened crust, or (b) because the compensated highlands overlie (or are drawn toward) current cold downwellings. Interpretation (a) is favored on the basis of geoid-topography admittance spectra for the highland plateaus, which show no evidence for long-wavelength dynamics beneath these regions [*Simons et al.*, 1997].

[33] 3. Although excluded from the active volcanic highlands proper, coronae are concentrated within a large area of Venus bounded by active highlands in the Beta-Atla-Themis ("BAT") region. The highlands themselves are commonly presumed to result from continuously active mantle plumes, due to the presence of large, uncompensated geoid highs and fresh volcanic constructions (review by *Smrekar et al.* [1997, and references therein] [*Simons et al.*, 1997]. Therefore the signatures of transient plumes (coronae) may be obliterated by continuous mantle plume activity in the active highlands (but see following sections for an alternative dynamical interpretation).

[34] 4. Coronae in the BAT region and other highland regions appear to constitute a "younger" population than those found in the lowlands, judging from the relative lack of uncompensated geoid highs and absence of pronounced fracture patterns in the latter population (Type 2 coronae). This supports inferences based on regional geological mapping of older coronae coeval with regional plains formation, and younger BAT coronae [*Chapman and Zimbelman*, 1998]. The more random distribution of the "older" coronae suggests that they may date from a time when modulation by the large-scale pattern of convection was weaker, or at least very different from that of the present time.

[35] These observations lead to a rough picture of Venus's internal dynamics as illustrated in the hypothetical cross section of Figure 7a. The location of this great circle cross sectional path is drawn for reference in Figure 1b (Venus's

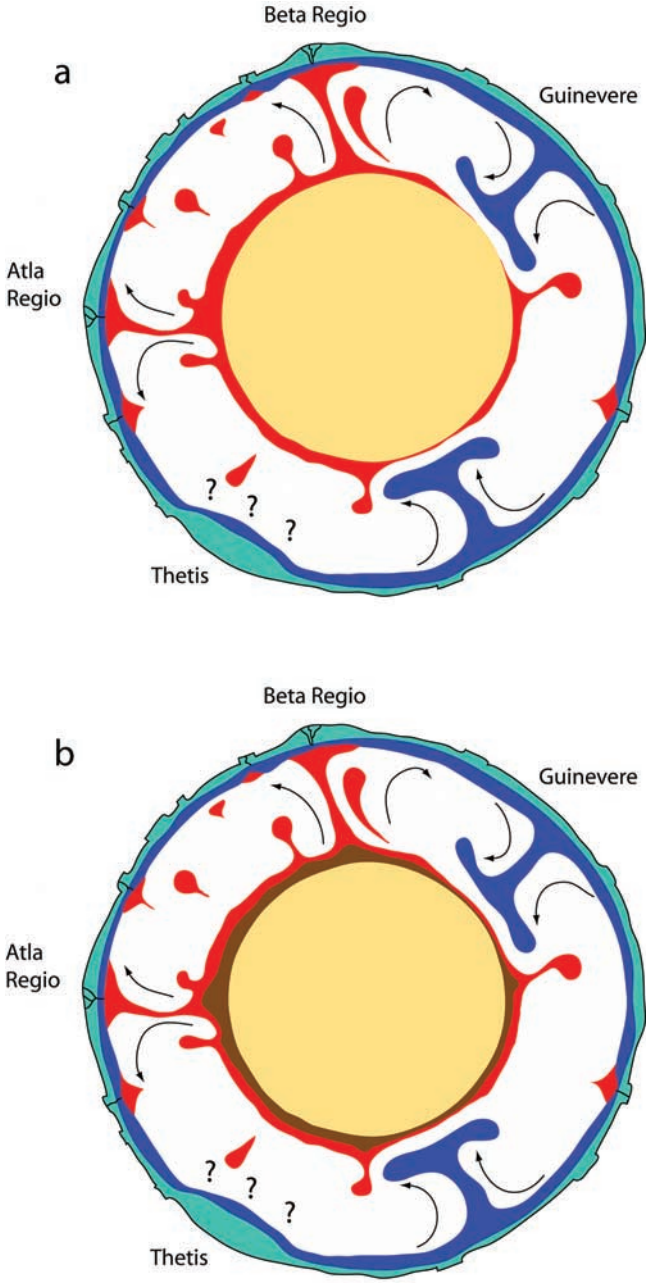

Figure 7. (a) Schematic cross-section through Venus determined by the plane of the great circle shown in Figure 1b. The cartoon illustrates the proposed current mantle dynamical regime of Venus suggested by a combination of the corona observations and laboratory experiments described in the text. Yellow, core; turquoise, crust; red, regions of positive thermal buoyancy; blue, regions of negative thermal buoyancy. (b) As in (a) but with the inclusion of a chemical boundary layer in the core-mantle boundary region (brown).

geoid). We choose this path to best illustrate the important inferred relations between surface tectonics and internal dynamics. Although the details of this cartoon are guided by convection theory (especially near the core-mantle boundary), it is important to emphasize that its main features are derived directly from the above list of observations. In the following sections, we attempt to interpret this phenomenological tapestry in light of recent studies of mantle convection.

6. Mantle Convection and the Tectonic Styles of the Terrestrial Planets

[36] The lithospheres of the terrestrial planets are the upper thermal boundary layers for mantle convection, which is thought to be very vigorous and time dependent for Earth and Venus, but less so for Mars and the Moon due mainly to their smaller radii. This convection is driven by some combination of internal radioactive decay and secular cooling. Because active thermal upwellings and downwellings result from boundary layer instabilities, uncertainties in heat source distribution, not to mention uncertainties regarding the existence of internal (thermo-chemical) boundary layers, make it difficult, a priori, to predict the importance of hot, upwelling plumes relative to cold (lithospheric), downwelling structures in determining the styles or patterns of mantle convection in the terrestrial planets.

[37] For Earth, a conservative view has been that the mantle heat flux supplied by the core due to secular cooling (and carried by plumes to form hot spots) is of order 10%, while the main mantle circulation is associated with the cooling and sinking (subduction) of oceanic lithosphere, driven mainly by radioactive heat production in the mantle [e.g., *Davies and Richards*, 1992]. Although Earth and Venus are of similar bulk composition and size, their differing thermo-chemical evolution may have resulted in very different distributions of internal heat sources. The apparent lack of plate tectonics on Venus, the association of volcanic highlands with large, uncompensated geoid signals, and the presence of coronae all suggest a prominent role for mantle plumes in the internal dynamics and tectonics of Venus. The apparent youth of Venus's surface implied by cratering studies [*McKinnon et al.*, 1997] suggests that Venus underwent a transition from a period of rapid and significant resurfacing to a period of much slower resurfacing. Unresolved issues include the rate of decline in average resurfacing rate [*Schaber et al.*, 1992; *Hauck et al.*, 1998], the style of mantle convection and surface tectonics prior to the transition [*Phillips and Hansen*, 1998; *Turcotte*, 1993; *Turcotte et al.*, 1999], and whether periods of intense lithospheric recycling are episodic and/or representative of Venus's long-term style of convection (see below).

[38] There has been considerable progress recently in understanding possible modes of lithospheric response to mantle convection. Regardless of the role of plumes in transporting heat from the core (or internal boundary layers), lithospheric (tectonic) style is probably dominated by rheological effects, i.e., the variation in effective mantle viscosity and failure strength with temperature, pressure, composition, and strain rate.

[39] The most important effect is that of temperature-dependent viscosity, which introduces a major asymmetry into thermal convection, such that the cold upper boundary layer may effectively become a "stagnant lid" to convection [e.g., *Christensen and Harder*, 1991; *Solomatov*, 1995]. This asymmetry means that only the lowermost part of the thermal boundary (lithosphere) participates in convective flow and that strain rates at the upper surface are negligibly

small. Since the effect of temperature on the creep strength (viscosity) of mantle rocks is enormous (orders of magnitude), the stagnant lid mode of convection is to be expected in an otherwise uncomplicated planet. This mode of convection has apparently held for Mars since its early history and also for the post-mare history of the Moon; however, neither Earth's or Venus's tectonic responses to mantle convection can be explained in such simple terms.

[40] A second important effect is that of lithospheric failure, associated with rheological mechanisms such as fracture and plasticity. When an effective yield strength is exceeded, strain rates increase rapidly, the extreme example being that of faults. Recent studies by a number of workers, particularly *Moresi and Solomotov* [1998] in application to Venus, have explored the dynamics of convection with combined temperature-dependent viscosity and failure rheology in the lithosphere. In two-dimensional, Cartesian, numerical models, this combination (with largely internal heating) results in three distinct styles of convection. For yield strengths large compared to the characteristic stresses due to convection, stagnant lid convection results, as expected. For low yield strengths, the asymmetry is largely broken and the lithosphere becomes continuously mobile, also as expected. An intermediate yield strength transitional mode of ''episodic overturn'' is characterized by short bursts of rapid motions of the entire lithosphere (accompanied by high heat flow) and separated by long periods of relative stagnation (low heat flow) [*Weinstein and Olson*, 1992; *Moresi and Solomatov*, 1998]. The lithosphere thickens until it is unstable, at which point it yields plastically, sinks, and cools the interior, all in cyclic fashion. This episodic overturn mode has been suggested to apply to Venus, with rapid resurfacing about 700–800 million years ago, followed by greatly reduced lithospheric motions [*Reese et al.*, 1999]. Stable plate-like motions are not obtained from a combined temperature-dependent viscosity/failure type of model, although during episodic overturn some regions of the lithosphere do behave in plate-like fashion [*Trompert and Hansen*, 1998].

[41] The third effect is that of a low-viscosity zone (LVZ) beneath the lithosphere. *Bunge et al.* [1996, 1997] showed that an LVZ of perhaps 1–2 orders of magnitude viscosity reduction results in a surprisingly long-wavelength pattern of downwelling sheets in otherwise simple convection models, suggesting that an LVZ promotes a long-linear downwelling style of convection as on Earth. *Tackley* [2000] and *Richards et al.* [2001] have more recently shown (in both 2-D and 3-D models) that when an LVZ is combined with a *Moresi-Solamotov* type temperature-dependent failure rheology in the lithosphere, very stable, plate-like, surface motions result for ''intermediate'' choices of lithospheric yield stress (i.e., yield stresses comparable to the viscous stresses due to internal convection).

[42] Taken altogether, the modeling work described above suggests that on Earth, either water or partial melting in the upper mantle (which may, of course, be related) are responsible for an LVZ, thus allowing plate tectonics to arise in a range of parameter space that otherwise results in alternation between stagnant and mobile lid behavior (Venus?). Evidence for the lack of an LVZ on Venus [e.g., *Kiefer et al.*, 1986], perhaps due to a lack of water, might therefore explain why Venus lacks plate tectonics. On Earth, cooling and sinking of the entire lithosphere dominates surface tectonics. On Venus, the main lithospheric downwelling involves only the lower portion of the lithosphere during the ''stagnant'' portion of its cycle, and presently occurs mainly beneath the Venusian lowlands with little consequent surface tectonic signature other than broad topographic depression [*Simons et al.*, 1997].

7. Upwelling Plumes

[43] The nature of mantle plumes on Earth is controversial. Here, we give a brief description of hot, upwelling plumes at high Rayleigh number (appropriate for Venus and Earth) and with temperature-dependent viscosity, followed by a brief account of new experimental work on the interaction of upwelling plumes with larger-scale flow structures and the lithosphere.

[44] The lower left-hand panel of Figure 8 shows a shadowgraph of typical plume head-and-tail forms that result from pure bottom heating (no top cooling) in a tank of corn syrup [see, e.g., *Lithgow-Bertelloni et al.*, 2001; *Jellinek et al.*, 2003]. The effective Rayleigh number here is modest ($\sim 10^6$), and the plumes become smaller, more numerous, and more transient in nature as the Rayleigh number is increased (middle and upper left-hand panels of Figure 8). These images contain much of our ''classical'' notion of plumes: Narrow, hot, low-viscosity, roughly axisymmetric conduits feed spherical plume heads that rise through the ambient fluid. However, this notion is a vastly oversimplified model with respect to mantle convection, where top cooling produces complementary downwellings that may alter the nature of these plumes in significant ways. Currently, there are no fully 3-D, high Rayleigh number simulations of mantle convection with strongly temperature-dependent viscosity, significant bottom heating, and surface plate-like motions. In the following section, we draw upon results from simpler laboratory experiments.

[45] The characteristic time and length scales for upwelling plumes are straightforward to estimate either theoretically or from laboratory-derived scalings [e.g., *Griffiths and Campbell*, 1990; *Lithgow-Bertelloni et al.*, 2001; *Jellinek et al.*, 2003], but uncertainties in the relevant parameters for the interiors of either Earth or Venus yield a wide range of plausible values, due mainly to uncertainties in estimates for viscosity. Flood basalts may require plume head diameters of order 300–1000 km [*Richards et al.*, 1989; *Campbell and Griffiths*, 1990; *Coffin and Eldholm*, 1993], while the plume tails responsible for hot spot tracks could range from tens to several hundred kilometers. Plume risetimes through the mantle are equally hard to constrain, and could range from a few million to $\sim$100 million years for either Venus or Earth.

[46] In a given regime of convection, characteristic plume dimensions and timescales are expected to fall in a rather restricted range. For Earth, we observe that large flood basalt events are often followed by narrow hot spot tracks, seeming to indicate two distinct length-scales (heads and tails), with the onset of new plume activity occurring perhaps every 10 million years or so [*Hill*, 1991]. Venus's coronae, along with supposed present-day plumes underlying the BAT highlands, immediately present a very

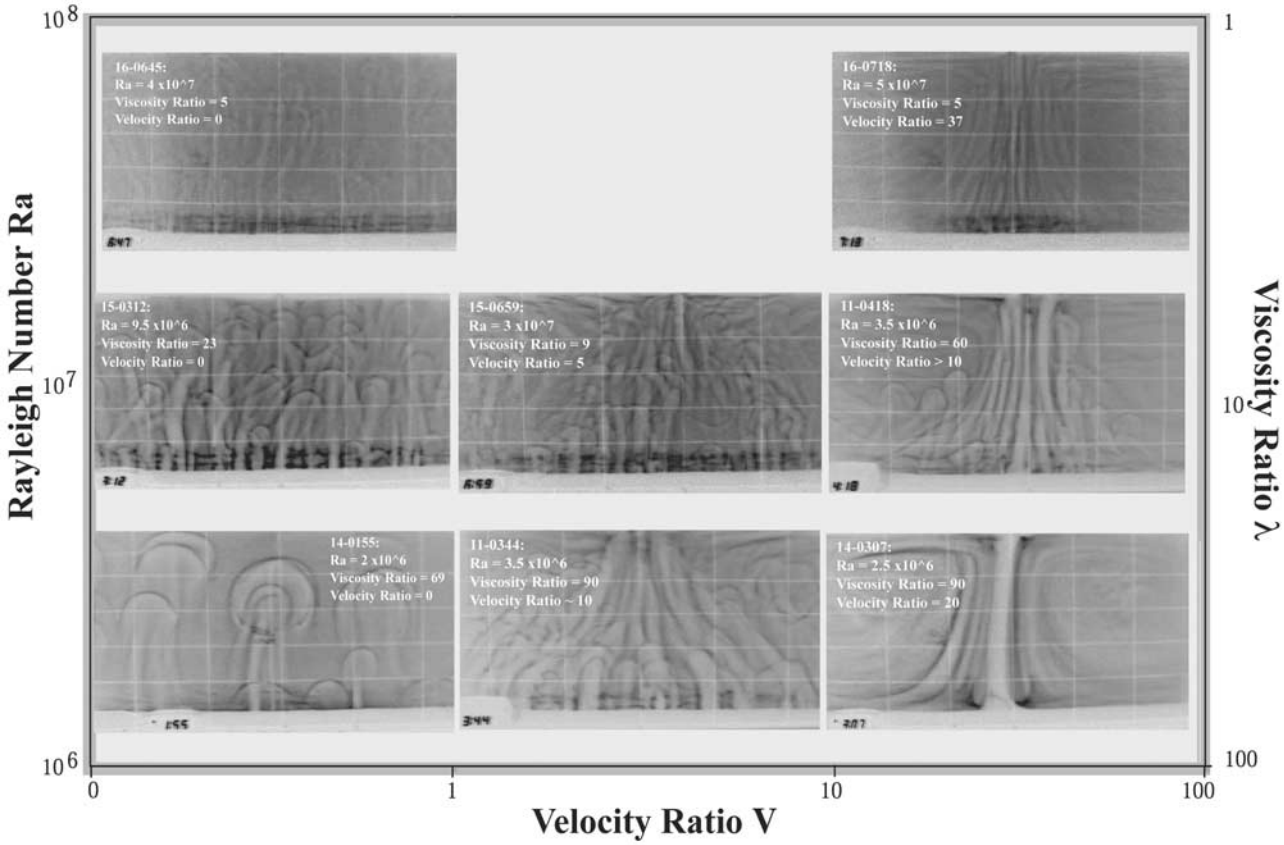

Figure 8. Shadowgraphs showing how plume formation and rise varies as a function of Rayleigh number, viscosity ratio across the lower thermal boundary layer, and imposed large-scale flow (horizontal velocities). The placement of the photographs is approximate and highly schematic. Because the experiments involve secular heating in time, and constant imposed large-scale flow velocity, the Rayleigh number increases and the viscosity contrast decreases in time during an experiment. The horizontal axis gives the ratio of the flow velocity imposed by conveyor belts at the top of the tank to the natural characteristic plume rise velocity. The actual horizontal advection velocities at the bottom of the tank are much smaller than those imposed at the top (due in part to the no-slip boundary), so that the velocity ratio at the bottom boundary layer is considerably smaller than indicated [from *Jellinek et al.*, 2003].

different picture: The coronae span a large and continuous range of diameters (less than 60 km to perhaps 2500 km) and appear to represent transient phenomena, while the geodynamically active highlands represent large and presumably long-lived thermal structures in the mantle.

[47] Another important aspect of the fluid mechanics is the effect of temperature-dependent viscosity on plumes. In stagnant lid convection, most of the temperature contrast, and hence viscosity contrast, occurs across the cold, stiff, top boundary layer. *Jellinek et al.* [2002] have recently pointed out that this might explain the abundance of transient plumes on Venus relative to Earth: For Earth, subduction of the entire lithosphere should lead to a larger temperature contrast across the core-mantle boundary than would normally occur in stagnant lid convection. The increased viscosity contrast tends to stabilize plume conduits [*Jellinek et al.*, 2002]. Upwelling plumes of lower viscosity contrast arising in stagnant lid convection (or during the ''stagnant'' phase of episodic convection) are likely more transient in nature. Under conditions of moderate viscosity contrast and fairly high Rayleigh number ($\sim 10^7$), transient plumes and stable plume conduits may coexist [*Lithgow-Bertelloni et al.*, 2001; *Weeraratne and Manga*, 1998], although the conditions under which this coexistence may occur are neither well-documented nor well-understood.

[48] Evidence for mantle plumes on Earth, Venus, and Mars suggests starkly differing plume modes. On Mars, there may be one true ''megaplume'' beneath Tharsis that has dominated Martian mantle convection and waned significantly (at least in terms of melt production) over the past several billion years. On Earth, plumes apparently play a secondary role in heat transport and melt production [*Sleep*, 1990; *Davies*, 1988], but their distribution also appears governed by a very large-scale mode of convection as discussed above, even though some of Earth's well-established hot spot plumes appear to suffer remarkably little effect from overlying plate motions [*Richards and Griffiths*, 1988]. Venus appears even more complicated, with multiple scales and two distinct modes of plume behavior. In the next section, we suggest that these modes might be explained in terms of specific types of plume/lithosphere and plume/

plume interactions that have been studied in recent fluid mechanical experiments.

8. Interacting Scales of Mantle Flow

[49] Neither laboratory nor numerical experiments have fully simulated the fluid mechanical conditions for solid-state convection in the interiors of Earth or Venus. Rayleigh numbers approaching 10^8 have been achieved in laboratory experiments with bottom heating and top cooling [*Davaille and Jaupart*, 1993; *Weeraratne and Manga*, 1998], using sugar syrups that have temperature-dependent viscosity. Fluid mechanical experiments have also been conducted to study the dynamics of buoyant plumes or thermals in isolation [e.g., *Whitehead and Luther*, 1975; *Olson and Singer*, 1985; *Griffiths*, 1986; *Richards and Griffiths*, 1988, 1989; *Griffiths and Campbell*, 1990; *Kincaid et al.*, 1995; *Feighner and Richards*, 1995], and such experiments form much of the basis for the current hot spot/mantle plume paradigm for Earth.

[50] Two recent series of laboratory experiments at high Rayleigh number appear relevant to interpreting the observations summarized above for the distribution of coronae on Venus. The first series was carried out in large convection tanks designed to study the formation of plumes at very high Rayleigh number ($10^6 - 10^9$) and the interactions of plumes with large-scale flow. *Lithgow-Bertelloni et al.* [2001] studied plume generation from a hot, bottom boundary layer (no top cooling) using a corn syrup with strongly temperature-dependent viscosity. Transient plume head-and-tail structures formed in stochastic fashion from the hot boundary layer, with plume characteristics (size, frequency) evolving predictably with the thickness and viscosity contrast across the boundary layer as the tank underwent secular heating. Steady upwelling conduits persisted in the flow as well, reflecting two distinct coexisting modes of plume-like heat transport. The steady plumes formed in the center of a broad-scale central upwelling in the convection tank driven by a small degree of cooling from the tank sidewalls. Furthermore, the transient plume instabilities (thermals) were also focused toward the large-scale upwelling flow, as a natural consequence of boundary layer thickening in response to the flow. Unfortunately, the data from these experiments were insufficient to further analyze this dual-mode plume behavior.

[51] Subsequent experiments have studied the concentration of upwelling plumes by controlled, large-scale flow [*Jellinek et al.*, 2003]. In addition to bottom heating, a large-scale flow was imposed by two opposing conveyor belts, producing a central, hot, upwelling sheet and complementary downwelling sheets at the sidewalls, with little cooling from either the top or sidewalls. For strongly temperature dependent viscosity, and for imposed large-scale flow velocities comparable to or greater than the ''natural'' transient plume rise velocities, the upwelling sheets captured much of the hot, low-viscosity boundary layer. Also, the heat flux from the boundary layer was largely captured by the large-scale flow for large-scale flow velocities comparable to plume rise velocities. Unless the large-scale flow velocity greatly exceeded the plume rise velocity, transient plumes (thermals) also persisted and were focused toward the large-scale upwelling flow.

[52] Figure 8 summarizes the regimes of plume-large-scale flow interactions found in these experiments. Imposed large-scale flow velocity increases from left to right. Rayleigh number increases (and viscosity contrast decreases) from bottom to top. At bottom left, plumes are unaffected by imposed large-scale flow, while at bottom right plumes are entirely suppressed by large-scale flow as most of the heat flow across the bottom boundary layer is captured by the pronounced central upwelling. The coexistence of a strong (induced) central upwelling from the boundary layer with transient plume instabilities is most apparent in the middle-right panel of Figure 8, where larger plume rise velocities (higher Rayleigh number) and somewhat smaller viscosity contrast lead to intermediate behavior, i.e., incomplete plume capture. Individual plume instabilities are completely captured in the immediate vicinity of the central upwellings.

[53] These results suggest that the transient plumes (thermals) that give rise to the BAT corona province may be concentrated by the large-scale mantle flow due to large Beta - Atla - Themis upwelling plume structures. The lack of coronae on the highland rises themselves may result from burial by continuous volcanic flows, but perhaps a more likely explanation is that nearby transient plumes are simply captured by the large, continuous plumes underlying the highlands. Similar reasoning may explain the relative paucity of hot spots near fast spreading ridges on Earth [*Jellinek et al.*, 2003].

[54] Another distinct series of experiments was performed by Manga and colleagues [*Weeraratne and Manga*, 1998; *Manga and Weeraratne*, 1999; *Schaeffer and Manga*, 2001]. These experiments are more classical in nature, involving high Rayleigh number convection in a temperature-dependent fluid with bottom heating and top cooling, and concentrating on the spatial and temporal characteristics of instabilities from both the top and bottom boundary layers and their interactions. *Schaeffer and Manga* [2001] found that for high Rayleigh number ($>10^7$) convection, unsteady, cold, downwelling plumes form within the lower part of the upper boundary layer (stagnant lid) with a frequency in time and with a characteristic spacing expected from simple boundary layer theory [*Howard*, 1966]. In other words, the cold and stiff upper boundary layer behaves almost independently of the lower boundary layer. In contrast, the hot, low-viscosity lower boundary layer generates plumes (thermals) with a higher characteristic frequency and smaller spacing, as expected, but also with a frequency and spacing imposed by the cold downwelling plumes (i.e., multiple time and length scales). The reason for this asymmetry is that the cold, stiff upper boundary layer is only weakly affected by hot, low-viscosity plumes, while the lower boundary layer is strongly modulated by the impingement of cold, stiff downwellings.

[55] A qualitative summary of these results is given in Figure 9, taken directly from *Schaeffer and Manga* [2001]. The smaller length and timescales for hot plume (thermal) formation, relative to the cold downwellings, is noteworthy. The downwellings nucleating beneath the stagnant lid occur at length scales comparable to the depth of the fluid, similar to the dimensions of Venus's lowlands, relative to mantle depth. However, the upwelling plumes form with a frequency

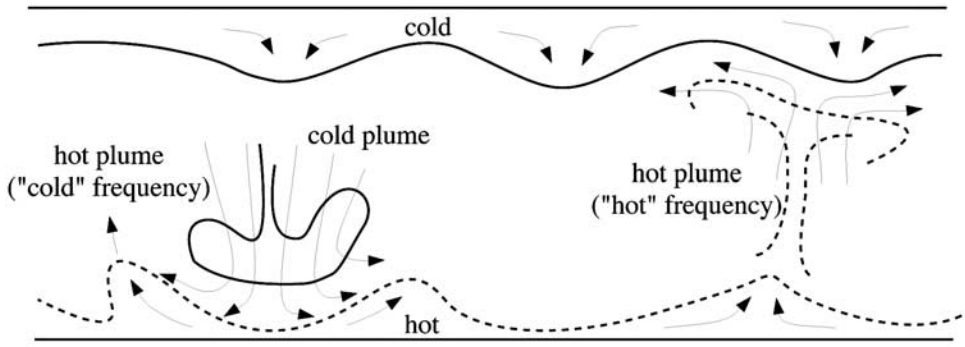

Figure 9. Interacting scales of flow for experiments with upper (cool) and lower (hot) thermal boundary layers. Cold downwellings are stiff and strongly modulate the locations and frequency of upwelling plumes from the hot lower boundary layer. In contrast, hot, low-viscosity upwellings exert little influence on the cold upper boundary layer [from *Schaeffer and Manga*, 2001].

at least double that of the downwellings and with a characteristic spacing perhaps several times smaller. (Individual hot thermals may impinge repeatedly near the same position at the surface, as implied by well-known tight clusters of coronae on Venus.)

[56] These results suggest that coronae on Venus are naturally excluded from lowland regions (volcanic plains), with the lowlands corresponding to dynamic downwelling structures (''drips'') from Venus's lithosphere [*Simons et al.*, 1997]. Interestingly, the experiments of *Weeraratne and Manga* [1998] also indicated the coexistence of persistent, or long-lived, plume conduits with more transient plume instabilities in the range of 10^7 Rayleigh number, similar to the regime observed by *Lithgow-Bertelloni et al.* [2001], although persistent conduits may not be present at higher Rayleigh numbers (M. Manga, private communication, 2002).

[57] These new experiments form a new, albeit incomplete, fluid mechanical framework for interpreting the relationship between upper boundary layer (lithosphere) dynamics and rising plumes from a lower (or internal) thermal boundary layer. The main results of relevance to our observations regarding Venus's coronae are (1) that small transient plume instabilities (coronae) may coexist with and be focused toward large, persistent plumes (Atla Regio, Beta Regio), and (2) that cold downwellings underlying the low-lying volcanic plains likely suppress or deflect the smaller-scale instabilities that cause coronae.

9. Layered Convection?

[58] An important caveat is that our discussion has been cast entirely in terms of thermal convection, neglecting the possibility of compositional layering of Venus's mantle. For Earth, compositional layering seems required at least in the lowermost mantle (D″). For Venus, there is no direct (i.e., seismic or geochemical) evidence for mantle layering, but it is reasonable to presume that some kind of dense layer may also exist at the base of, or within, Venus's mantle.

[59] Recent laboratory and numerical experiments have begun to shed some light on the influences of such a layer on transient plume formation [e.g., *Davaille*, 1999a, 1999b; *Tackley*, 1998; *Jellinek and Manga*, 2002; *Gonnermann et al.*, 2002]. One certain effect is the thickening of the dense layer beneath large-scale upwelling structures, as indicated in the cartoon of Figure 7b. Deep thermal plumes from such an elevated boundary layer may, among many other possible effects, be stabilized by coupling between these layers [*Jellinek and Manga*, 2002]. It is also possible that Venus (perhaps unlike Earth) has developed more pronounced internal layering than Earth (perhaps due to a lack of stirring across the endothermic spinel/perovskite phase boundary by stiff subducted plates [see, e.g., *Zhong and Gurnis*, 1994]). Such layering could lead to multiple scales of plume activity [*Davaille*, 1999a; *Gonnermann et al.*, 2002], which is a possibility that merits further investigation.

10. Summary Interpretation of the Distribution of Coronae on Venus

[60] We now return to interpreting the four principal observed associations of coronae with tectonic provinces and internal dynamics on Venus. Because the picture from numerical and experimental fluid mechanics is incomplete, some of our interpretations remain conjecture, at least in part, and so generate hypotheses for examination in future studies. To the four points stated previously, we also add a fifth addressing the thorny issue of the size distribution (variation in radii) of coronae, which in turn will imply a new interpretation of the physical mechanism responsible for coronae:

[61] 1. The exclusion of coronae, especially those that may be tectonically and volcanically younger, from the broad lowland plains likely results from the suppression of plume instabilities beneath active downwellings of Venus's lithosphere. The experiments of *Schaeffer and Manga* [2001] explain the long-wavelength nature of these lowland downwellings relative to the smaller size and closer spacing of the much more numerous coronae. In this interpretation, the coronae represent highly transient, detached thermals, and stagnant lid convection limits viscosity contrast across the lower boundary layer [*Jellinek et al.*, 2002]. In Figure 7, we have sketched the downwellings arbitrarily as continuous structures, since cold stiff plumes tend more toward that morphology, but it is possible that these structures are also more transient and detached.

[62] 2. We offer no new insight into the exclusion of coronae from compensated highlands, and either thickened

crust or associated downwelling structures remain plausible explanations.

[63] 3. Transient plume instabilities (thermals) are focused toward large-scale upwelling flow because of both lower boundary layer thickening and horizontal advection of plumes in the large-scale flow. Thermals that approach the large-scale upwelling are ''captured''; hence coronae are excluded from the immediate vicinity of active highlands, while being concentrated toward broad-scale active upwelling (BAT region). (Note that here, as earlier, the term ''active'' means that gravity/topography admittances are consistent with support of topography by dynamic normal stresses at the base of the lithosphere.) We caution, however, that the suggestive experimental work by *Jellinek et al.* [2003] is for imposed sheet-like upwelling structures and that the observed coexistence of steady plume conduits and more transient thermals [*Lithgow-Bertelloni et al.*, 2001] needs further study and documentation. Nonetheless, a further implication, or hypothesis, is that the effective Rayleigh number governing plume convection in Venus may lie near a transitional value of order 10^7.

[64] 4. That the abundant BAT coronae appear to be younger than the relatively few coronae occurring in the lowlands suggests that the latter may have formed before the present-day lowland downwelling structures became fully developed. Thus there may have been a transition in both the frequency (increasing in time) and spatial distribution (becoming less random in time) of coronae formation during the last billion years or so.

[65] 5. Thermals tend to form with a relatively narrow size (diameter) distribution in a given regime of convection, whereas Venus's coronae exhibit a remarkably broad range of sizes, in terms of both fracture patterns and topography. We believe the likely reason for this disparity is that coronae are caused mainly by melt intrusion rather than thermal uplift of the lithosphere due to transient plumes. Small variations in plume temperature and lithospheric thickness (melting depth) may cause very large variations in melt production as plumes impinge beneath the lithosphere [e.g., *McKenzie and Bickle*, 1988]. This idea is developed further by *Dombard et al.* [2002; manuscript in preparation, 2003], who demonstrate that thermal uplift stresses due to the impingement of the transient plume are likely insufficient to cause the characteristic lithospheric failure (faulting) for even larger coronae. Instead, ponding of primary melt at the crust/mantle boundary or at a level of neutral density within the crust prior to fractionation and (sometimes) eruption offers a quantitatively plausible cause of fracturing and uplift. In this model, the variation in coronae diameter reflects variations in the diameter (and perhaps depth) of melt intrusion, which is likely smaller (but possibly larger as well) than the thermal width of the flattened plume at the base of the lithosphere, depending again on conditions of temperature and pressure for melting. This new hypothesis needs to be tested further, but we know of no other plausible explanations for the great variation in corona diameter, if one assumes that coronae are associated with transient plumes. The mechanism proposed by *Dombard et al.* [2002] contrasts with that of *Tackley and Stevenson* [1993], who suggested that melt diapirs may be generated within large-scale mantle upwellings. The latter mechanism invokes a self-perpetuating partial melting instability, and might explain the clustering of many coronae above a broad mantle upwelling beneath the BAT province. The *Dombard et al.* [2002] model, in contrast, does not necessarily invoke a single BAT-scale upwelling. *Nimmo and McKenzie* [1996] have considered the effect of melt buoyancy in large, continuous plumes as a source of dynamic uplift and gravity anomalies associated with some highland structures. However, the majority of coronae have likely been caused by transient plumes, and we believe that the tectonism and volcanism associated with them are due mainly to the effects of shallow melt intrusion.

11. Hypotheses Regarding the Evolution of Venus

[66] These interpretations invoke ''mixed'' regimes of thermal convection in Venus's interior, i.e., the coexistence of steady plumes (active volcanic highlands) with more transient plumes or thermals (coronae). Although coronae may represent an important mode of internal heat transport (perhaps of order 25% the total mantle heat flux [*Smrekar and Stofan*, 1997]), they may also function somewhat as the proverbial canary in the coal mine in delineating the large-scale structure and evolution of Venus over the past billion years.

[67] Two possible implications are immediately apparent: (1) The frequency of occurrence of coronae may be increasing in time, perhaps due to an effective Rayleigh number increase as Venus's mantle warms and as effective viscosity contrast across the lower boundary layer decreases, in the wake of a transition from mobile to stagnant lid convection. Both effects serve to promote more time-dependent plume activity [*Lithgow-Bertelloni et al.*, 2001; *Jellinek et al.*, 2002]. (2) The large-scale upwelling and downwelling structures of Venus may have developed relatively recently (perhaps also following a mobile/stagnant-lid transition). This notion could explain why the ''older'' coronae are more scattered, whereas the ''younger'' coronae are concentrated in upwelling regions and excluded from downwelling regions.

[68] Several other hypotheses for recent transitions in the dynamics of Venus have been suggested. *Turcotte* [1993] suggested episodic and catastrophic overturn because of an endothermic phase transition, based on 2-D convection simulations. However, 3-D numerical convection simulations have shown that this mechanism is much weaker than previously thought [*Tackley et al.*, 1994; *Bunge et al.*, 1996, 1997]. *Herrick* [1994] and *Phillips and Hansen* [1998] both suggested a secular transition from mobile to stagnant lid convection, and *Reese et al.* [1999] suggested a pervasive mantle melting event in response to late onset of sublithospheric convection. None of these scenarios, however, addressed either the role of coronae or their possible utility in distinguishing among possible models.

[69] It is our view that neither the current level of theoretical understanding of mantle convection nor the current base of geological and geophysical observations are sufficient to explain the recent evolution of Venus. It is hopefully clear from the above discussion of laboratory convection studies where improvements are needed: Particular attention needs to be devoted to understanding the possible coexistence of steady and highly transient plumes, and transitions between such regimes, and, of course, much

more work is needed to better establish the rheological controls on the various lithospheric/tectonic regimes (mobile, stagnant lid, transitional, plate-like). The effects of chemical density stratification on plume formation are just beginning to be explored.

[70] We also emphasize the importance of additional observations from geological mapping, which would further understanding of the role of coronae in the thermal and tectonic evolution of Venus. First and foremost, better relative timing constraints on corona formation and evolution would constrain models for the recent evolution of mantle dynamics on Venus. The hypotheses we have advanced suggest that the chronology of coronae emplacement might shed much light on large-scale dynamics as well. Laboratory experiments to date suggest that an increase in effective Rayleigh number for Venus's mantle should result in an increase in the formation of thermals and their resulting surface structures: coronae. Can further study of relative ages of coronae permit any regional or global test of this hypothesis? An associated complication is whether there is evidence for even partial burial of "older" coronae due to volcanism from either nearby younger coronae or other volcanic sources. Of particular interest is whether there has been burial of coronae in the topographic lowlands. Are we able to test whether coronae in the lowland or plains regions are indeed older, on average, than coronae in the BAT region?

[71] Observations of the spatial distributions of subsets of the corona population, and new laboratory plume experiments, have led us to focus how coronae may elucidate Venus's mantle convective regime over the last ~750 Myr. We have alluded only briefly to models for corona formation and evolution; however, understanding in detail the mechanism of corona formation is critical to understanding the surprisingly large range in corona attributes such as size, relief, gravity signatures, tectonic expression, and volcanism.

[72] Our conceptual model does not require corona-forming upwellings to originate at a mid-mantle interface [e.g., *Smrekar and Stofan*, 1999]. Instead, coronae can form as a natural consequence of thermal transients that arise from the deep mantle and cause melting in the uppermost mantle, in analogy to the surface volcanic manifestation of terrestrial hot spots. Such a model for corona formation, emphasizing the role of melt intrusion and fractionation, is further explored by *Dombard et al.* [2002; manuscript in preparation, 2003]. Volcanic, tectonic, and topographic differences among coronae may reflect differences in interior temperatures of transient plumes, depths of melting, and local crustal and lithospheric thicknesses. Further investigations of such models for corona formation are needed in order to test the overall conceptual model we have presented here.

[73] **Acknowledgments.** This work was supported under NASA grants NAG5-4620 and NAG5-11563. Both authors gratefully acknowledge the Carnegie Institution of Washington for visiting appointments during 2000 and 2001 that facilitated this research. Preliminary analyses contributing to this study were conducted by Sarah Zimmerman. We thank Ellen Stofan for early access to the expanded corona data set and also Sean Solomon, Steve Hauck, Roger Phillips and Jon Aurnou for helpful discussions. An anonymous review greatly improved the clarity of the manuscript and the discussion of the statistical results. We especially acknowledge Andrew Dombard for many discussions and for reviews of early and revised versions of the manuscript. Mark Jellinek and Helge Gonnermann kindly shared their new experimental work on interactions of plumes and large-scale flow in advance of publication.

References

Addington, E. A., A stratigraphic study of small volcano clusters on Venus, *Icarus*, *149*, 16–36, 2001.

Barsukov, V. L., et al., Preliminary evidence on the geology of Venus from radar measurements by the Venera 15 and 16 probes, *Geokhimia*, *12*, 111–120, 1984. (*Geochem. Int.*, Engl. Transl., *22*, 135–143, 1985).

Barsukov, V. L., et al., The geology and geomorphology of the Venus surface as revealed by the radar images obtained by Veneras 15 and 16, *J. Geophys. Res.*, *91*, 378–398, 1986.

Basilevsky, A. T., and J. W. Head, Onset time and duration of corona activity on Venus: Stratigraphy and history from photogeological study of stereo images, *Earth Moon Planets*, *76*, 67–115, 1998.

Basilevsky, A. T., J. W. Head, G. G. Schaber, and R. G. Strom, The resurfacing history of Venus, in *Venus II*, edited by S. W. Brougher, D. M. Hunten, and R. J. Phillips, pp. 1047–1085, Univ. of Ariz. Press, Tucson, 1997.

Bills, B. G., W. S. Kiefer, and R. L. Jones, Venus gravity: A harmonic analysis, *J. Geophys. Res.*, *92*, 10,335–10,351, 1987.

Bunge, H. P., M. A. Richards, and J. R. Baumgardner, The effect of depth-dependent viscosity on the planform of mantle convection, *Nature*, *379*, 436–438, 1996.

Bunge, H. P., M. A. Richards, and J. R. Baumgardner, A sensitivity study of 3-D spherical mantle convection at 10^8 Rayleigh number: Effects of depth-dependent viscosity, heating mode, and an endothermic phase change, *J. Geophys. Res.*, *102*, 11,991–12,007, 1997.

Campbell, B. A., Surface formation rates and impact crater densities on Venus, *J. Geophys. Res.*, *104*, 21,951–21,956, 1999.

Campbell, I. H., and R. W. Griffiths, Implications of mantle plume structure for the evolution of flood basalts, *Earth Planet. Sci. Lett.*, *99*, 79–83, 1990.

Chapman, M. A., and J. R. Zimbelman, Corona associations and their implications for Venus, *Icarus*, *132*, 344–361, 1998.

Christensen, U., and H. Harder, Convection with variable viscosity, *Geophys. J. Int.*, *104*, 213–226, 1991.

Coffin, M. F., and O. Eldholm, Scratching the surface: Estimating dimensions of large igneous provinces, *Geology*, *21*, 515–518, 1993.

Copp, D. L., J. E. Guest, and E. R. Stofan, Stratigraphy of six coronae on Venus: Implications for timing and sequence of corona formation, *J. Geophys. Res.*, *103*, 19,410–19,418, 1998.

Crough, S. T., and D. M. Jurdy, Subducted lithosphere, hotspots, and the geoid, *Earth Planet. Sci. Lett.*, *48*, 15–22, 1980.

Davaille, A., Simultaneous generation of hotspots and superswells by convection in a heterogeneous planetary mantle, *Nature*, *402*, 756–760, 1999a.

Davaille, A., Two-layer thermal convection in miscible viscous fluids, *J. Fluid Mech.*, *379*, 223–253, 1999b.

Davaille, A., and C. Jaupart, Transient high-Rayleigh-number thermal convection with large viscosity variations, *J. Fluid Mech.*, *253*, 141–166, 1993.

Davies, G. F., Ocean bathymetry and mantle convection, 1, Large-scale flow and hotspots, *J. Geophys. Res.*, *93*, 10,467–10,480, 1988.

Davies, G. F., and M. A. Richards, Mantle convection, *J. Geol.*, *100*, 151–206, 1992.

Dombard, A. J., C. L. Johnson, M. R. Richards, and S. C. Solomon, A transient plume melting model for coronae on Venus, *Lunar Planet. Sci.* [CD-ROM], *XXXIII*, abstract 1877, 2002.

Feighner, M. A., and M. A. Richards, The fluid dynamics of plume-ridge and plume-plate interactions: An experimental investigation, *Earth Planet. Sci. Lett.*, *129*, 171–182, 1995.

Ford, P. G., and G. H. Pettengill, Venus topography and kilometer-scale slopes, *J. Geophys. Res.*, *97*, 13,103–13,114, 1992.

Glaze, L. S., E. R. Stofan, S. E. Smrekar, and S. M. Baloga, Insights into corona formation through statistical analyses, *J. Geophys. Res.*, *107*(E12), 5135, doi:10.1029/2002JE001904, 2002.

Gonnermann, H. M., M. Manga, and A. M. Jellinek, Dynamics and longevity of an initially stratified mantle, *Geophys. Res. Lett.*, *29*(10), 1399, doi:10.1029/2002GL014851, 2002.

Griffiths, R. W., The differing effects of compositional and thermal buoyancies on the evolution of mantle diapirs, *Phys. Earth Planet. Inter.*, *43*(4), 261–273, 1986.

Griffiths, R. W., and I. H. Campbell, Stirring and structure in mantle plumes, *Earth Planet. Sci. Lett.*, *99*, 66–78, 1990.

Guest, J. E., and E. R. Stofan, A new view of the stratigraphic history of Venus, *Icarus*, *139*, 55–66, 1999.

Hansen, V. L., Venus diapirs: Thermal or compositional?, *Geol. Soc. Am. Bull.*, in press, 2003.

Hansen, V. L., J. J. Willis, and W. B. Banerdt, Tectonic overview and synthesis, in *Venus II*, pp. 797–844, Univ. of Ariz. Press, Tucson, 1997.

Hauck, S. A., R. J. Phillips, and M. H. Price, Venus: Crater distribution and plains resurfacing models, *J. Geophys. Res.*, *103*, 13,635–13,642, 1998.

Herrick, R. R., Resurfacing history of Venus, *Geology*, *22*, 703–706, 1994.

Herrick, R. R., and R. J. Phillips, Geological correlations with interior density structure of Venus, *J. Geophys. Res.*, *97*, 16,017–16,034, 1992.

Hill, R. I., Starting plumes and continental breakup, *Earth Planet. Sci. Lett.*, *104*, 398–416, 1991.

Howard, L. N., Convection at high Rayleigh number, in *Proceedings of the 11th International Congress of Applied Mechanics*, edited by H. Gortler, pp. 1109–1115, Springer-Verlag, New York, 1966.

Janes, D. M., S. W. Squyres, D. L. Bindschadler, G. Baer, G. Schubert, V. L. Sharpton, and E. R. Stofan, Geophysical models for the formation and evolution of coronae on Venus, *J. Geophys. Res.*, *97*, 16,055–16,068, 1992.

Jellinek, A. M., and M. Manga, The influence of a chemical boundary layer on the fixity, spacing, and lifetime of mantle plumes, *Nature*, *418*(6899), 760–763, 2002.

Jellinek, A. M., A. Lenardic, and M. Manga, The influence of interior mantle temperature on the structure of plumes: Heads for Venus, Tails for the Earth, *Geophys. Res. Lett.*, *29*(11), 1532, doi:10.1029/2001GL014624, 2002.

Jellinek, A. M., H. M. Gonnermann, and M. A. Richards, Plume capture by divergent plate motions: Implications for the distribution of hotspots, geochemistry of mid-ocean ridge basalts, and estimates of the heat flux at the core-mantle boundary, *Earth Planet. Sci. Lett.*, *205*(3–4), 361–378, 2003.

Johnson, C. L., and S. C. Solomon, A global gravity study of coronae on Venus, *Lunar Planet. Sci.* [CD-ROM], *XXXIII*, abstract 1952, 2002.

Johnson, C. L., E. Hargrave, M. Simons, and S. C. Solomon, Old and young coronae on Venus: Combining regional and global studies to constrain thermal evolution models, *Lunar Planet. Sci.*, *XXVIII*, 665–666, 1997.

Kiefer, W. S., M. A. Richards, B. H. Hager, and B. G. Bills, A dynamic model of Venus's gravity field, *Geophys. Res. Lett.*, *13*, 14–17, 1986.

Kincaid, C., G. Ito, and C. Gable, Laboratory investigation of the interaction of off-axis mantle plumes and spreading centers, *Nature*, *376*, 758–761, 1995.

Koch, D. M., and M. Manga, Neutrally buoyant diapers—A model for Venus coronae, *Geophys. Res. Lett.*, *23*, 225–228, 1996.

Konopliv, A. S., W. B. Banerdt, and W. L. Sjogren, Venus gravity: 180th degree and order model, *Icarus*, *134*, 3–18, 1999.

Lithgow-Bertelloni, C., M. A. Richards, R. W. Griffiths, and C. P. Conrad, Plume generation in natural thermal convection at high Rayleigh and Prandtl numbers, *J. Fluid Mech.*, *434*, 1–21, 2001.

Manga, M., and D. Weeraratne, Experimental study of non-Boussinesq Rayleigh-Benard convection at high Rayleigh and Prandtl numbers, *Phys. Fluids*, *11*, 2969–2976, 1999.

McKenzie, D., The relationship between gravity and topography on Earth and Venus, *Icarus*, *112*, 55–84, 1994.

McKenzie, D., and M. J. Bickle, The volume and composition of melt generated by extension of the lithosphere, *J. Petrol.*, *29*, 625–679, 1988.

McKinnon, W. B., K. J. Zahnle, B. A. Ivanov, and H. J. Melosh, Cratering on Venus: Models and observations, in *Venus II*, pp. 969–1014, Univ. of Ariz. Press, Tucson, 1997.

Moresi, L., and V. Solomatov, Mantle convection with a brittle lithosphere: Thoughts on the global tectonic styles of the Earth and Venus, *Geophys. J. Int.*, *133*, 669–682, 1998.

Namiki, N. S., and S. Solomon, Impact crater densities on volcanoes and coronae on Venus: Implications for volcanic resurfacing, *Science*, *265*, 929–933, 1994.

Nimmo, F., and D. McKenzie, Modelling plume-related uplift, gravity and melting on Venus, *Earth Planet. Sci. Lett.*, *145*, pp. 109–123, 1996.

Olson, P., and H. Singer, Creeping plumes, *J. Fluid Mech*, *158*, 511–531, 1985.

Parmentier, E. M., and P. C. Hess, Chemical differentiation of a convecting planetary interior: Consequences for a one plate planet such as Venus, *Geophys. Res. Lett.*, *19*, 2015–2018, 1992.

Phillips, R. J., Estimating lithospheric properties at Atla Regio, Venus, *Icarus*, *112*, 147–170, 1994.

Phillips, R. J., and V. L. Hansen, Geological evolution of Venus: Rises, plains, plumes, and plateaus, *Science*, *279*, 1492–1497, 1998.

Phillips, R. J., and M. C. Malin, The interior of Venus and tectonic implications, in *Venus*, pp. 159–214, Univ. of Ariz. Press, Tucson, 1983.

Phillips, R. J., R. F. Raubertas, R. E. Arvidson, I. C. Sarkar, R. R. Herrick, N. Izenberg, and R. E. Grimm, Impact craters and Venus resurfacing history, *J. Geophys. Res.*, *97*, 15,923–15,948, 1992.

Phillips, R. J., C. L. Johnson, S. J. Mackwell, P. Morgan, D. T. Sandwell, and M. Zuber, Lithospheric mechanics and dynamics of Venus, in *Venus II*, edited by S. W. Bougher, D. M. Hunten, and R. J. Phillips, pp. 1163–1204, Univ. of Ariz. Press, Tucson, 1997.

Press, W. H., B. R. Flannery, S. A. Teukolsky, and W. T. Vettering, *Numerical Recipes*, Cambridge Univ. Press, New York, 1989.

Price, M., and J. Suppe, Mean age of rifting and volcanism on Venus deduced from impact crater densities, *Nature*, *372*, 756–759, 1994.

Price, M. H., G. Watson, J. Suppe, and C. Brankman, Dating volcanism and rifting on Venus using impact crater densities, *J. Geophys. Res.*, *101*, 4657–4671, 1996.

Rappaport, N. J., A. S. Konopliv, and A. B. Kucinskas, An improved 360 degree and order model of Venus topography, *Icarus*, *134*, 19–31, 1999.

Reese, C. C., V. S. Solomatov, and L.-N. Moresi, Non-Newtonian stagnant lid convection and magmatic resurfacing on Venus, *Icarus*, *139*, 67–80, 1999.

Richards, M. A., and D. C. Engebretson, Large-scale mantle convection and the history of subduction, *Nature*, *355*, 437–440, 1992.

Richards, M. A., and R. W. Griffiths, Deflection of plumes by mantle shear flow: Experimental results and a simple theory, *Geophys. J. Int.*, *94*, 367–376, 1988.

Richards, M. A., and R. W. Griffiths, Thermal entrainment by deflected mantle plumes, *Nature*, *342*, 900–902, 1989.

Richards, M. A., B. H. Hager, and N. H. Sleep, Dynamically supported geoid highs over hotspots: Observation and theory, *J. Geophys. Res.*, *93*, 7690–7780, 1988.

Richards, M. A., R. A. Duncan, and V. E. Courtillot, Flood basalts and hotspot tracks: Plume heads and tails, *Science*, *246*, 103–107, 1989.

Richards, M. A., W.-S. Yang, J. R. Baumgardner, and H.-P. Bunge, Role of a low-viscosity zone in stabilizing plate tectonics: Implications for comparative terrestrial planetology, *Geochem. Geophys. Geosyst.*, *2*, Paper number 2000GC000115, 2001.

Schaber, G. G., R. G. Strom, H. J. Moore, L. A. Soderblom, R. L. Kirk, D. J. Chadwick, D. D. Dawson, L. R. Gaddis, J. M. Boyce, and J. Russell, Geology and distribution of impact craters on Venus: What are they telling us?, *J. Geophys. Res.*, *97*, 13,257–13,302, 1992.

Schaeffer, N., and M. Manga, Interaction of rising and sinking mantle plumes, *Geophys. Res. Lett.*, *28*, 455–458, 2001.

Simons, M., S. C. Solomon, and B. H. Hager, Localization of gravity and topography: Constraints on the tectonics and mantle dynamics of Venus, *Geophys. J. Int.*, *131*, 24–44, 1997.

Sleep, N. H., Hotspots and mantle plumes: Some phenomenology, *J. Geophys. Res.*, *95*, 6715–6736, 1990.

Smrekar, S., Evidence of active hotspots on Venus from analysis of Magellan gravity data, *Icarus*, *112*, 2–26, 1994.

Smrekar, S. E., and E. R. Stofan, Coupled upwelling and delamination: A new mechanism for corona formation and heat loss on Venus, *Science*, *277*, 1289–1294, 1997.

Smrekar, S. E., and E. R. Stofan, Origin of corona-dominated rises on Venus, *Icarus*, *139*, 100–115, 1999.

Smrekar, S. E., W. S. Kiefer, and E. R. Stofan, Large volcanic rises on Venus, in *Venus II*, edited by S. W. Bougher, D. M. Hunten, and R. J. Phillips, pp. 845–878, Univ. of Ariz. Press, Tucson, 1997.

Solomatov, V. S., Scaling of temperature-dependent and stress-dependent viscosity convection, *Phys. Fluids*, *7*, 266–274, 1995.

Squyres, S. W., D. M. Janes, G. Baer, D. L. Bindschadler, G. Schubert, V. L. Sharpton, and E. R. Stofan, The morphology and evolution of coronae on Venus, *J. Geophys. Res.*, *97*, 13,611–13,634, 1992.

Stofan, E. R., et al., Global distribution and characteristics of coronae and related features on Venus: Implications for origin and relation to mantle processes, *J. Geophys. Res.*, *97*, 13,347–13,378, 1992.

Stofan, E. R., V. E. Hamilton, D. M. Janes, and S. E. Smrekar, Coronae on Venus, in *Venus II*, edited by S. W. Bougher, D. M. Hunten, and R. J. Phillips, pp. 931–965, Univ. of Ariz. Press, Tucson, 1997.

Stofan, E. R., S. E. Smrekar, S. W. Tapper, J. E. Guest, and P. M. Grindrod, Preliminary analysis of an expanded corona database for Venus, *Geophys. Res. Lett.*, *28*, 4267–4270, 2001.

Strom, R. G., G. G. Schaber, and D. D. Dawson, The global resurfacing of Venus, *J. Geophys. Res.*, *99*, 10,899–10,926, 1994.

Tackley, P. J., Three-dimensional simulation of mantle convection with a thermo-chemical boundary layer: D″, in *The Core-Mantle Boundary Region*, *Geodyn. Ser.*, vol. 28, edited by M. Gurnis et al., pp. 231–253, AGU, Washington, D. C., 1998.

Tackley, P. J., Self-consistent generation of tectonic plates in time-dependent, three-dimensional mantle convection simulations, 2, Strain weakening and asthenosphere, *Geochem. Geophys. Geosyst.*, *1*, Paper number 2000GC000043, 2000.

Tackley, P. J., and D. J. Stevenson, A mechanism for spontaneous self-perpetuating volcanism on the terrestrial planets, in *Flow and Creep in the Solar System*, edited by D. B. Stone and S. K. Runcorn, pp. 307–321, Kluwer Acad., Norwell, Mass., 1993.

Tackley, P. J., D. J. Stevenson, G. A. Glatzmaier, and G. Schubert, Effects of phase transitions in three-dimensional spherical models of convection in Earth's mantle, *J. Geophys. Res.*, *99*, 15,887–15,901, 1994.

Trompert, R. A., and U. Hansen, Mantle convection simulations with rheologies that generate plate-like behavior, *Nature*, *395*, 686–689, 1998.

Turcotte, D. L., An episodic hypothesis for Venusian tectonics, *J. Geophys. Res.*, *98*, 17,061–17,068, 1993.

Turcotte, D. L., G. Morein, D. Roberts, and B. D. Malamud, Catastrophic resurfacing and episodic subduction on Venus, *Icarus*, *139*, 49–54, 1999.

Watson, G. S., A test for randomness, *Mon. Not. R. Astron. Soc.*, *7*, 160–161, 1956.

Weeraratne, D., and M. Manga, Transitions in the style of mantle convection at high Rayleigh numbers, *Earth Planet. Sci. Lett.*, *160*, 563–568, 1998.

Weinstein, S. A., and P. L. Olson, Thermal convection with non-Newtonian plates, *Geophys. J. Int.*, *111*, 515–530, 1992.

Whitehead, J. A., and D. S. Luther, Dynamics of laboratory diapir and plume models, *J. Geophys. Res.*, *80*, 705–717, 1975.

Zhong, S., and M. Gurnis, Role of plates and temperature-dependent viscosity in phase change dynamics, *J. Geophys. Res.*, *99*, 15,903–15,917, 1994.

Zhong, S. J., and M. Gurnis, Mantle convection with plates and mobile, faulted plate margins, *Science*, *267*, 838–843, 1995.

Zimmerman, S., and C. L. Johnson, Gravity signatures of coronae on Venus: Implications for models for corona formation and evolution, *Eos Trans. AGU*, Spring Meet. Suppl., *81*(19), abstract P61A-05, 2000.

C. L. Johnson, Institute of Geophysics and Planetary Physics, Scripps Institution of Oceanography, 9500 Gilman Drive, La Jolla, CA 92093-0225, USA. (johnson@igpp.ucsd.edu)

M. A. Richards, Department of Earth and Planetary Science, University of California, Berkeley, Berkeley, CA 94270, USA.